

國立臺灣大學工學院化學工程學系



碩士論文

Department of Chemical Engineering  
College of Engineering  
National Taiwan University  
Master Thesis

球形帶電軟質粒子懸浮液中之電泳可動度及導電度  
Electrophoretic Mobility and Effective Electric  
Conductivity of Concentrated Suspensions of Charged  
Soft Spheres

劉軒僑

Hsuan-Chiao Liu

指導教授：葛煥彰教授

Advisor: Huan-Jang Keh, Professor

中華民國 一百零五 年 六 月

June, 2016

國立臺灣大學碩士學位論文  
口試委員會審定書

球形帶電軟質粒子懸浮液中之電泳可動度及導電度

Electrophoretic Mobility and Effective Electric Conductivity of  
Concentrated Suspensions of Charged Soft Spheres

本論文係劉軒僑君 (R03524088) 在國立臺灣大學化學工程學系  
所完成之碩士學位論文，於民國 105 年 6 月 17 日承下列考試委員審  
查通過及口試及格，特此證明

口試委員：

葛煥利

(簽名)

(指導教授)

張有義

詹正傑

系主任、所長

王大銘

(簽名)

## 誌謝



能夠順利完成這篇論文，首先我要感謝我的指導教授 葛教授煥彰先生。感謝老師在我還未進入實驗室時，就給予我充分的指導，讓我能夠在投入研究後，快速進入狀況。在研究過程中，每當遇到困難時，老師都會耐心指導我，並且明確指出問題所在，使我能夠快速克服阻礙。老師除了擁有淵博的專業知識和清晰的邏輯能力外，還有嚴謹的研究態度，這些不僅讓我在學習上受益良多，也讓我做事態度和面對困難上成長許多，在此由衷感謝老師的辛勞付出。同時，也感謝口試委員張有義教授以及詹正雄教授，謝謝他們在論文上的校閱和審核，並且給予我許多珍貴的意見和想法，使得本論文更加充實。

再來，我要感謝實驗室的學長、同學以及學弟們。感謝泰成學長在我剛進入實驗室時給予各方面的協助；謝謝冠宇學長教導我研究工具的使用，並且在我研究初期耐心指導，讓我在研究上少走許多冤枉路；謝謝弘憲學長，提供我研究以外生活上的幫助，讓我能更快適應新的環境；謝謝馨妘學姐指導我研究上的各種問題，並且在研究上相似處給予我重要的幫助；謝謝家齊學長，帶給實驗室許多歡樂；謝謝同學瑋哲，在研究和課業上都給我很大的幫助，尤其在研究上的互相討論，讓我的研究事半功倍；謝謝同學漢章，時常一起討論課業上的問題，並且在實驗室的大小事中給我各種幫助；謝謝學弟正彥以及建賢，分享研究以外的經驗和趣事，讓研究生生活更加有趣。

最後，我要感謝我的家人，謝謝爸爸媽媽從小到大的付出，讓我能在沒有其他負擔下專心完成我的碩士學位，並且分享他們自身的經驗讓我在碩士學位這條路上走得更加順利，謝謝我的家人成就今日的我。

謹以此論文，獻給我的家人以及所有幫助過我的朋友們。

民國 一百零五年 六月

劉軒僑

# 摘要



本論文使用單元小室模型複合粒子是由帶有固定表面電荷密度 $\sigma$ ，半徑為 $r_0$ 之球形固體核心以及其表面吸附一帶有固定空間電荷密度 $Q$ ，厚度為 $a-r_0$ 之溶液可穿透多孔層所構成。藉由探討處理此懸浮系統中之靜電力和電動力方程式，可以獲得複合粒子電泳可動度和懸浮液導電度之解析解，並在任意的 $r_0/a$ ， $\lambda a$ ， $\kappa a$ 和粒子於懸浮液中之體積分率值的情況下，以 $\sigma$ 和 $Q$ 的線性關係式表示，其中 $\lambda$ 為多孔層布林克曼滲透長度之倒數， $\kappa$ 為電雙層德拜屏蔽長度之倒數，這些粒子表面吸附層的特性及粒子間的交互作用等參數對於粒子電泳可動度和懸浮液導電度有著顯著且複雜的影響。本研究除了獲得複合粒子懸浮液中之電泳可動度和導電度結果外，也可在 $r_0 = a$ 和 $r_0 = 0$ 的極限下，分別簡化成為球形硬質粒子和多孔粒子之特例結果，這些結果對於分析相關實驗數據資料有所幫助。

關鍵字：電泳，有效導電度，軟質粒子，濃懸浮液，單元小室模型

# Abstract



A thorough analytical study of the electrophoresis and electric conduction in a suspension of charged soft particles in an arbitrary electrolyte solution is presented through the use of a unit cell model. Each soft particle is a spherical hard core of radius  $r_0$  and constant surface charge density  $\sigma$  covered with a permeable porous layer of constant thickness  $a - r_0$  and uniform fixed charge density  $Q$ . Solving the relevant electrostatic and electrokinetic differential equations, we obtain closed-form formulas for the electrophoretic mobility of the soft particles and effective electric conductivity of the suspension. These results are expressed as linear functions of  $\sigma$  and  $Q$  for arbitrary values of  $r_0/a$ ,  $\lambda a$ ,  $\kappa a$ , and the particle volume fraction of the suspension, where  $\lambda$  is the reciprocal of the Brinkman permeation length of the surface layer of each particle, and  $\kappa$  is the reciprocal of the Debye screening length. The effects of the surface layer characteristics and particle interactions on the electrophoretic mobility and effective conductivity are interesting, significant, and complicated. The general results for a suspension of charged soft spheres, which reduce to those of hard spheres and porous spheres in the limits  $r_0 = a$  and  $r_0 = 0$ , respectively, provide valuable information for interpreting experimental data.

Keywords: Electrophoresis, Effective electric conductivity, Soft sphere, Concentrated suspension, Unit cell model



# Table of Contents



摘要 .....	I
Abstract .....	II
List of Figures .....	VI
<b>Chapter 1 Introduction</b> .....	<b>1</b>
<b>Chapter 2 Solution for the Potential and Flow Fields</b> .....	<b>4</b>
2.1 Electric Potential Field .....	5
2.2 Electrochemical Potential Energy Field .....	7
2.3 Fluid Flow Field .....	9
<b>Chapter 3 Solution for the Electrophoretic Velocity and Electric Conductivity</b> .....	<b>12</b>
3.1 Electrophoretic Velocity .....	12
3.2 Electric Conductivity .....	13

<b>Chapter 4</b>	<b>Results and Discussion.....</b>	<b>15</b>
4.1	Suspension of Hard Spheres.....	15
4.2	Suspension of Porous Spheres.....	19
4.3	Suspension of Soft Spheres.....	22
<b>Chapter 5</b>	<b>Concluding Remarks.....</b>	<b>41</b>
	<b>List of Symbols.....</b>	<b>43</b>
	<b>References.....</b>	<b>46</b>
<b>Appendix</b>	<b>The constants <math>C_{ni}</math> in Eqs. (29) and (30).....</b>	<b>49</b>
	<b>Biographical Sketch.....</b>	<b>65</b>

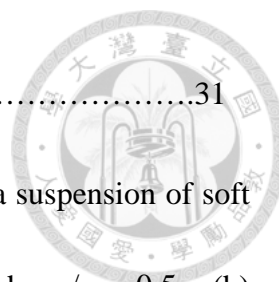




# List of Figures



- Figure 1.** Geometric sketch for a charged soft sphere in a unit cell under an imposed electric field. ....11
- Figure 2.** Plots of the normalized electrophoretic mobility  $U_1$  for a suspension of hard spheres as calculated from Eq. (36) versus the parameters  $\kappa a$  and  $\varphi$ . The solid and dashed curves represent the calculations for the Happel and Kuwabara models, respectively. ....25
- Figure 3.** Plots of the electric conductivity parameter  $X_1$  for a suspension of hard spheres as calculated from Eq. (41) versus the parameters  $\kappa a$  and  $\varphi$ . The solid and dashed curves represent the calculations from using the Dirichlet condition in Eq. (12a) and Neumann condition in Eq. (12b), respectively. ....27
- Figure 4.** Plots of the normalized electrophoretic mobility  $U_2$  for a suspension of porous spheres as calculated from Eq. (36) versus the parameters  $\kappa a$  and  $\varphi$  for the Happel model. The solid and dashed curves represent the calculations with  $\lambda a = 5$  and  $\lambda a = 20$ , respectively. ....29
- Figure 5.** Plots of the electric conductivity parameter  $X_2$  for a suspension of porous spheres as calculated from Eq. (49) versus the parameters  $\kappa a$  and



$\varphi$  .....31

**Figure 6.** Plots of the electrophoretic mobility parameter  $U_1$  for a suspension of soft spheres as calculated from Eq. (36): (a)  $\varphi = 0.1$  and  $r_0/a = 0.5$ ; (b)  $\kappa a = 1$  and  $\lambda a = 1$ . The solid and dashed curves represent the calculations for the Happel and Kuwabara models, respectively. ....33

**Figure 7.** Plots of the electrophoretic mobility parameter  $U_2$  for a suspension of soft spheres as calculated from Eq (36): (a)  $\varphi = 0.1$  and  $r_0/a = 0.5$ ; (b)  $\kappa a = 1$  and  $\lambda a = 1$ . The solid and dashed curves represent the calculations for the Happel and Kuwabara models, respectively. ....35

**Figure 8.** Plots of the electric conductivity parameter  $X_1$  for a suspension of soft spheres as calculated from Eq. (40) or (41): (a)  $r_0/a = 0.5$ ; (b)  $\kappa a = 1$ . The solid and dashed curves represent the calculations from using the Dirichlet condition in Eq. (12a) and Neumann condition in Eq. (12b), respectively. ....37

**Figure 9.** Plots of the electric conductivity parameter  $X_2$  for a suspension of soft spheres as calculated from Eq. (40): (a)  $r_0/a = 0.5$ ; (b)  $\kappa a = 1$ . The solid and dashed curves represent the calculations from using the Dirichlet condition in Eq. (12a) and Neumann condition in Eq. (12b), respectively. ....39

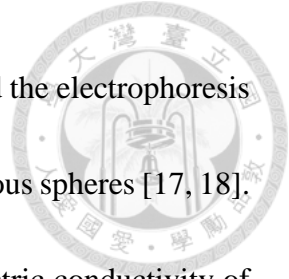
# Chapter 1

## Introduction



When an electric field is exerted on colloidal particles suspended in an electrolyte solution, the charged particles and neighboring counterions will move by electrophoresis and electric migration, respectively. As a result, the ambient fluid is dragged to flow, attended with an electric current. Some analytical expressions for the mean electrophoretic mobility of the particles and effective electric conductivity of the suspension have been obtained in the past for dilute suspensions of charged hard spheres (impermeable to the electrolyte solution) [1-4], porous spheres (permeable) [5, 6], and soft spheres (each is a hard spherical core of radius  $r_0$  covered with a porous surface layer of thickness  $a - r_0$ ) [7, 8]. In the limiting cases of  $r_0 = a$  and  $r_0 = 0$ , the results for the suspension of charged soft spheres reduce to those of hard spheres and porous spheres, respectively, of radius  $a$ .

In real situations of electrophoresis and electric conduction, relatively concentrated suspensions of charged particles are often involved, and a unit cell model may be used to estimate the effect of particle interactions. This model allows a homogeneous dispersion of particles to be divided into numerous identical cells, with one particle inhabiting at the center of each cell, and thus the multiple-particle problem is reduced to a single-particle



one for a cell. Adopting the cell model, many researchers investigated the electrophoresis and electric conduction in suspensions of hard spheres [9-16] and porous spheres [17, 18]. Experimental data for the electrophoretic mobility and effective electric conductivity of suspensions of charged particles [19-21] are in agreement with the predictions from the cell model in broad ranges of the volume fraction of the particles and the relative thickness of the electric double layers.

The electrophoresis in a concentrated suspension of soft spheres was also examined numerically or semi-analytically via the unit cell model to some extent [22-24], but the electrophoretic mobility and effective electric conductivity of concentrated suspensions of charged soft particles have not been thoroughly analyzed yet. In this thesis, the cell model is adopted to analytically study the electrophoresis and electric conduction in a suspension of generally charged soft particles. The linearized Poisson-Boltzmann/Laplace equations, continuity equation of ionic species, and Stokes/Brinkman equation modified with an electric force term are solved for the electric potential, ionic electrochemical potential energy, and fluid velocity fields, respectively, without any restrictions on the values of  $r_0/a$ ,  $\lambda a$ ,  $\kappa a$ , and the volume fraction of the particles, where  $\lambda$  is the Brinkman shielding coefficient in the surface porous layer of each particle and  $\kappa$  is the Debye screening parameter. Closed-form formulas for the electrophoretic mobility and effective electric conductivity of the suspension in terms of

the fixed charge densities of the particles are derived as Eqs. (35) and (38), respectively.



# Chapter 2

## Solution for the Potential and Flow Fields



We consider a suspension of soft spherical particles of radius  $a$  in a fluid solution of  $M$  ionic species. Each soft sphere is a charged hard core of radius  $r_0$  covered with a homogeneous, solvent-permeable, ion-penetrable, and charged porous layer of thickness  $a - r_0$ . When the suspension is subjected to an applied electric field  $E_\infty \mathbf{e}_z$ , where  $\mathbf{e}_z$  is the unit vector along the  $z$  axis, the particles undergo electrophoresis with a velocity  $U\mathbf{e}_z$  and an electric current passes through the suspension in the same direction. As shown in Fig. 1, we adopt a unit cell model in which each particle is located at the center of a spherical cell of radius  $b$  and  $\phi = (a/b)^3$  equals the particle volume fraction of the whole suspension. The origin of the spherical coordinates  $(r, \theta, \phi)$  is placed at the center of the cell and  $z = r \cos \theta$ . Thus, the problem in the cell is axially symmetric without  $\phi$  dependency.

To determine the electrophoretic velocity of the particles and the effective electric conductivity of the suspension at the steady state, we first need to find the distributions of the electric potential, electrochemical potential energy (or concentration) of each ionic species, and fluid flow field in the electrolyte solution within a cell in this chapter.



## 2.1. Electric potential field

The electric potential distribution  $\psi(r, \theta)$  in the fluid region between the rigid core of the soft particle and the outer (virtual) boundary of the cell ( $r_0 \leq r \leq b$ ) can be expressed as the equilibrium potential distribution  $\psi_{\text{eq}}(r)$  induced by the fixed charges of the particle and mobile ions in the surrounding electric double layer added with the perturbed potential distribution  $\psi_a(r, \theta)$  caused by the external electric field  $E_\infty \mathbf{e}_z$  [25, 26],

$$\psi = \psi_{\text{eq}} + \psi_a, \quad (1)$$

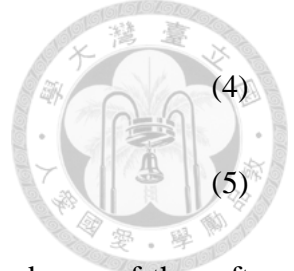
With employing the Debye-Hückel approximation at equilibrium, the electric potential  $\psi_{\text{eq}}$  is governed by the linearized Poisson-Boltzmann equation,

$$\nabla^2 \psi_{\text{eq}} = \kappa^2 \psi_{\text{eq}} - \frac{Q}{\varepsilon} h(r), \quad (2)$$

In this equation,  $\varepsilon$  is the dielectric permittivity of the fluid,  $Q$  is the fixed-charge density in the porous shell of the soft particle,  $h(r)$  is a step function equal to unity if  $r_0 \leq r < a$  (within the porous shell) and zero if  $a < r \leq b$ , and  $\kappa = e(\sum_{m=1}^M z_m^2 n_m^\infty / \varepsilon kT)^{1/2}$  is the Debye screening parameter, where  $n_m^\infty$  and  $z_m$  are the bulk concentration (number density) and valence, respectively, of the species  $m$ ,  $e$  is the elementary electric charge,  $k$  is the Boltzmann constant, and  $T$  is the absolute temperature.

The boundary conditions for the equilibrium potential are

$$r = r_0: \quad \frac{d\psi_{\text{eq}}}{dr} = -\frac{\sigma}{\varepsilon}, \quad (3)$$



$$r = a: \quad \psi_{\text{eq}} \text{ and } \frac{d\psi_{\text{eq}}}{dr} \text{ are continuous,} \quad (4)$$

$$r = b: \quad \frac{d\psi_{\text{eq}}}{dr} = 0, \quad (5)$$

where  $\sigma$  is the constant surface charge density of the dielectric hard core of the soft particle, which is related to the local equilibrium potential via the Gauss condition in Eq.

(3). Note that Eq. (5) for the unit cell allows the overlap of the electric double layers of adjacent particles.

The solution to Eqs. (2)-(5) can be obtained as

$$\psi_{\text{eq}} = \frac{1}{\varepsilon\kappa^2} [\psi_1(r)\kappa\sigma + \psi_2(r)Q] \quad (6)$$

where

$$\psi_1(r) = 2(\kappa r_0)^2 \frac{e^{\kappa(r_0+b)}}{B\kappa r} \{ \kappa b \cosh[\kappa(b-r)] - \sinh[\kappa(b-r)] \}, \quad (7)$$

$$\psi_2(r) = \frac{e^{-\kappa r}}{2B\kappa r} \{ [e^{\kappa a}(\kappa r_0 + 1)(\kappa a - 1) - e^{\kappa(2r_0-a)}(\kappa r_0 - 1)(\kappa a + 1)][e^{2\kappa b}(\kappa b - 1) + e^{2\kappa r}(\kappa b + 1)] \} \quad \text{for } a \leq r \leq b, \quad (8a)$$

$$\psi_2(r) = \frac{e^{\kappa(2b-a+2r_0-r)}}{2B\kappa r} \left\{ \frac{1}{B} - (\kappa b - 1)[\kappa a(\kappa r_0 - 1) + \kappa r_0] + \kappa b + e^{\kappa(a-2b)}(\kappa r_0 - 1)(\kappa b + 1) \right. \\ \left. \times [e^{\kappa a}(\kappa a - 1) - 2e^{\kappa r}\kappa r] + e^{\kappa(r-2r_0)}(\kappa r_0 + 1)(\kappa b - 1)[2e^{\kappa a}\kappa r - e^{\kappa r}(\kappa a + 1)] \right. \\ \left. + e^{2\kappa(a-b-r_0+r)}(\kappa r_0 + 1)(\kappa a - 1)(\kappa b + 1) \right\} \quad \text{for } r_0 \leq r \leq a, \quad (8b)$$

and

$$B = e^{2\kappa b}(\kappa r_0 + 1)(\kappa b - 1) - e^{2\kappa r_0}(\kappa r_0 - 1)(\kappa b + 1) \quad (9)$$

The potential  $\psi_a$  caused by the external electric field  $E_\infty \mathbf{e}_z$  satisfies the governing equation



$$\nabla^2 \psi_a = 0 \quad (10)$$

and boundary conditions

$$r = r_0: \quad \frac{\partial \psi_a}{\partial r} = 0, \quad (11)$$

$$r = b: \quad \psi_a = -E_\infty r \cos \theta \quad (\text{for the Dirichlet approach [10, 16]}), \quad (12a)$$

$$\frac{\partial \psi_a}{\partial r} = -E_\infty \cos \theta \quad (\text{for the Neumann approach [9, 11]}). \quad (12b)$$

Because the tangential component of the potential gradient at  $r = b$  is not specified in Eq. (12b), the Dirichlet approach in Eq. (12a) may be more logical than the Neumann approach.

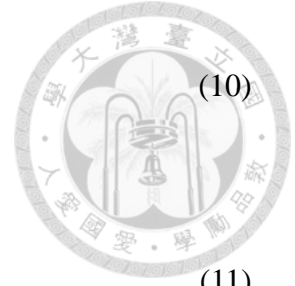
The solution to Eqs. (10)-(12) is

$$\psi_a = -\frac{E_\infty}{2\nu} \left(2 + \frac{r_0^3}{r^3}\right) r \cos \theta \quad (13)$$

where  $\nu = 1 + r_0^3/2b^3$  if Eq. (12a) is used and  $\nu = 1 - r_0^3/b^3$  if Eq. (12b) is employed. In the limiting case of  $r_0/b = 0$  ( $r_0 = 0$  or  $\varphi = 0$ ), Eqs. (12a) and (12b) lead to identical result (with  $\nu = 1$ ) as expected.

## 2.2. Electrochemical potential energy field

The electrochemical potential energy distribution  $\mu_m(r, \theta)$  of the species  $m$  (a linear combination of the ionic concentration  $n_m$  and perturbed potential  $\psi_a$ ) satisfies the continuity equation of the species [8]





$$\nabla^2 \mu_m = -\frac{z_m^2 e^2 E_\infty}{kT\nu} \left(1 - \frac{r_0^3}{r^3}\right) \frac{d\psi_{\text{eq}}}{dr} \cos \theta \quad (14)$$

and boundary conditions

$$r = r_0: \quad \frac{d\mu_m}{dr} = 0, \quad (15)$$

$$r = a: \quad \mu_m \text{ and } \frac{d\mu_m}{dr} \text{ are continuous,} \quad (16)$$

$$r = b: \quad \mu_m = -z_m e E_\infty r \cos \theta \text{ (if Eq. (12a) is used),} \quad (17a)$$

$$\frac{d\mu_m}{dr} = -z_m e E_\infty \cos \theta \text{ (if Eq. (12b) is used).} \quad (17b)$$

Using Eq. (6) for  $\psi_{\text{eq}}$  correct to the first orders of the fixed charge densities  $\sigma$  and

$Q$ , we obtain the solution to Eqs. (14)-(17) as

$$\mu_m = -\frac{E_\infty}{\nu} \left\{ z_m e \left(1 + \frac{r_0^3}{2r^3}\right) r + \frac{z_m^2 e^2 b}{\varepsilon \kappa^2 kT} [F_1(r) \kappa \sigma + F_2(r) Q] \right\} \cos \theta, \quad (18)$$

where

$$F_i(r) = \frac{-1}{6br^2} \left\{ [2r_0^3 I_{3i}(a, b) + b^3 I_{0i}(a, b)] \frac{2r^3 + r_0^3}{\nu b^3} + [2I_{3i}(r_0, a) + I_{0i}(r_0, a)] \frac{2(1-\nu)r^3 + r_0^3}{\nu} \right.$$

$$\left. + 2r_0^3 I_{3i}(a, r) - 2r^3 I_{0i}(a, r) \right\} \quad \text{for } a \leq r \leq b \quad (19a)$$

$$F_i(r) = \frac{-1}{6br^2} \left\{ [2r_0^3 I_{3i}(r_0, b) + b^3 I_{0i}(r_0, b)] \frac{2r^3 + r_0^3}{\nu b^3} + 2r_0^3 I_{3i}(r_0, r) - 2r^3 I_{0i}(r_0, r) \right\}$$

$$\text{for } r_0 \leq r \leq a, \quad (19b)$$

and

$$I_{ni}(r_1, r_2) = \int_{r_1}^{r_2} \left(1 - \frac{r_0^3}{r^3}\right) \left(\frac{r}{r_0}\right)^n \frac{d\psi_i}{dr} dr. \quad (20)$$

This result will be used in the next chapter to determine the effective electric conductivity

of the suspension of charged soft spheres.



### 2.3. Fluid flow field

The velocity field  $\mathbf{v}(r, \theta)$  and dynamic pressure distribution  $p(r, \theta)$  of the incompressible Newtonian fluid are governed by the following equation of continuity and Stokes/Brinkman equation with an electric force term:

$$\nabla \cdot \mathbf{v} = 0, \quad (21)$$

$$\nabla^2 \mathbf{v} - \lambda^2 h(r) \mathbf{v} = \frac{1}{\eta} (\nabla p - \varepsilon \kappa^2 \psi_{\text{eq}} \nabla \psi_a), \quad (22)$$

where  $\lambda$  is the Brinkman shielding coefficient, which is the reciprocal of a characteristic length for the flow penetration inside the porous shell of the soft particle, and  $\eta$  is the fluid viscosity.

We take the reference frame to travel with the particle in the cell and the boundary conditions for the fluid flow field as

$$r = r_0: \quad v_r = v_\theta = 0, \quad (23)$$

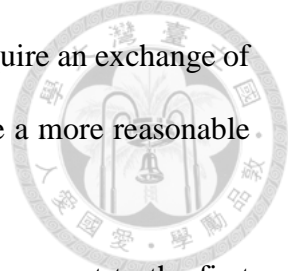
$$r = a: \quad v_r, v_\theta, \tau_{rr} - p, \text{ and } \tau_{r\theta} \text{ are continuous,} \quad (24)$$

$$r = b: \quad v_r = -U \cos \theta, \quad (25a)$$

$$\frac{\tau_{r\theta}}{\eta} = r \frac{\partial}{\partial r} \left( \frac{v_\theta}{r} \right) + \frac{1}{r} \frac{\partial v_r}{\partial \theta} = 0 \quad (\text{for the Happel model [27]}), \quad (25b)$$

$$[\nabla \times \mathbf{v}]_\phi = \frac{1}{r} \frac{\partial}{\partial r} (r v_\theta) - \frac{1}{r} \frac{\partial v_r}{\partial \theta} = 0 \quad (\text{for the Kuwabara model [28]}), \quad (25c)$$

where  $v_r$  and  $v_\theta$  are the nontrivial components of the fluid velocity,  $\tau_{rr}$  and  $\tau_{r\theta}$  are the nontrivial components of the viscous stress, and  $U$  is the electrophoretic velocity of



the particle to be determined. Because the Happel model does not require an exchange of mechanical energy between the cell and its environment, it might be a more reasonable approach than the Kuwabara model.

The solutions to Eqs. (21)-(25) together with Eqs. (6) and (13) correct to the first orders of the fixed charge densities  $\sigma$  and  $Q$  are

$$p = \frac{E_\infty}{\nu\kappa^2 a} [p_1(r)\kappa\sigma + p_2(r)Q] \cos \theta, \quad (26)$$

$$v_r = \frac{E_\infty}{\nu\eta\kappa^2} [v_{r1}(r)\kappa\sigma + v_{r2}(r)Q] \cos \theta, \quad (27)$$

$$v_\theta = -\frac{\partial(r^2 v_r)}{2r\partial r} \tan \theta, \quad (28)$$

where

$$p_i(r) = [C_{2i} + J_{3i}(r)]\left(\frac{a}{r}\right)^2 + 2[5C_{4i} + J_{0i}(r)]\frac{r}{a} - \kappa^2 ar\left(1 + \frac{r_0^3}{2r^3}\right)\psi_i(r), \quad (29a)$$

$$v_{ri}(r) = C_{1i} - J_{2i}(r) + [C_{2i} + J_{3i}(r)]\frac{a}{r} + [C_{3i} - \frac{1}{5}J_{5i}(r)]\left(\frac{a}{r}\right)^3 + [C_{4i} + \frac{1}{5}J_{0i}(r)]\left(\frac{r}{a}\right)^2$$

for  $a \leq r \leq b$ , (29b)

$$p_i(r) = \lambda^2 ar[-C_{5i} + \frac{C_{6i}}{2}\left(\frac{a}{r}\right)^3] + J_{3i}(r)\left(\frac{a}{r}\right)^2 + 2J_{0i}(r)\frac{r}{a} - \kappa^2 ar\left(1 + \frac{r_0^3}{2r^3}\right)\psi_i(r), \quad (30a)$$

$$v_{ri}(r) = C_{5i} + [C_{6i} + C_{7i}\alpha(\lambda r) + C_{8i}\beta(\lambda r)]\left(\frac{a}{r}\right)^3 - \frac{2}{(\lambda a)^2} [J_{0i}(r) - J_{3i}(r)]\left(\frac{a}{r}\right)^3$$

$$- 3J_{\alpha i}(r)\frac{\beta(\lambda r)}{(\lambda r)^3} + 3J_{\beta i}(r)\frac{\alpha(\lambda r)}{(\lambda r)^3} \quad \text{for } r_0 \leq r \leq a, \quad (30b)$$

$$J_{\alpha i}(r) = \frac{1}{6}(\kappa a)^2 \int_a^r \left(2 + \frac{r_0^3}{r^3}\right) \alpha(\lambda r) \frac{d\psi_i}{dr} dr, \quad (31a)$$

$$J_{\beta i}(r) = \frac{1}{6}(\kappa a)^2 \int_a^r \left(2 + \frac{r_0^3}{r^3}\right) \beta(\lambda r) \frac{d\psi_i}{dr} dr, \quad (31b)$$

$$J_{ni}(r) = \frac{1}{6}(\kappa a)^2 \int_a^r \left(2 + \frac{r_0^3}{r^3}\right) \left(\frac{r}{a}\right)^n \frac{d\psi_i}{dr} dr, \quad (31c)$$

$$\alpha(x) = x \cosh x - \sinh x, \quad (32a)$$

$$\beta(x) = x \sinh x - \cosh x, \quad (32b)$$

$i = 1$  and 2, and the dimensionless constants  $C_{ni}$  (independent of  $\sigma$ ,  $Q$ , and  $\nu$ ) for both the Happel and Kuwabara cell models are given by Eqs. (A1)-(A8) in the Appendix.

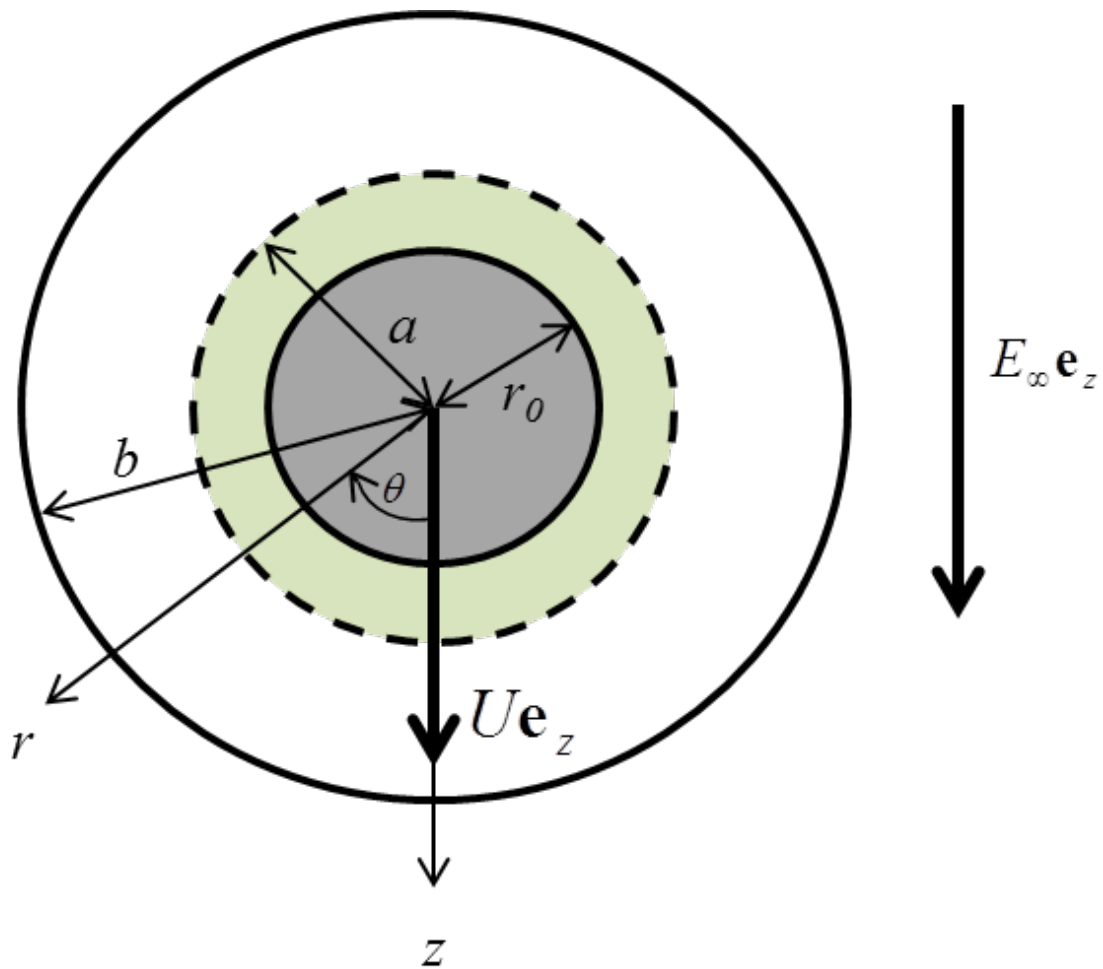
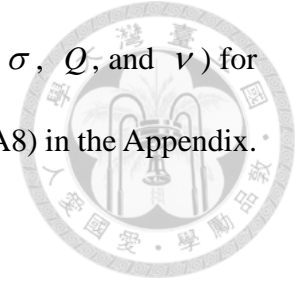


**Figure 1.** Geometric sketch for a charged soft sphere in a unit cell under an imposed electric field.



# Chapter 3

## Solution for the Electrophoretic Velocity and Electric Conductivity

### 3.1 Electrophoretic velocity

The net force exerted on the soft sphere is composed of the hydrodynamic force

$$\mathbf{F}_h = 2\pi a^2 \int_0^\pi \{(\tau_{rr} - p)\mathbf{e}_r + \tau_{r\theta}\mathbf{e}_\theta\} \sin\theta \, d\theta \quad (33)$$

and electrostatic force

$$\mathbf{F}_e = 2\pi a^2 \varepsilon \int_0^\pi \nabla \psi_{\text{eq}} \nabla \psi_a \cdot \mathbf{e}_r \sin\theta \, d\theta, \quad (34)$$

where  $\mathbf{e}_r$  and  $\mathbf{e}_\theta$  are the unit vectors in the  $r$  and  $\theta$  directions. This net force vanishes at the steady state. The application of this constraint after the substitution of Eqs. (6), (13), and (26)-(30) into Eqs. (33) and (34) results in the electrophoretic velocity of the particle as

$$U = \frac{E_\infty a}{v\eta} (U_1 \sigma + U_2 a Q), \quad (35)$$

where

$$U_i = \frac{J_{2i}(b)}{(\kappa a)^i} + \frac{1}{(\kappa a)^i A_0} \left\{ \frac{A_1}{6} [(\kappa a)^2 (2 + \frac{r_0^3}{a^3}) \psi_i(a) - 6a \frac{d\psi_i}{dr}(a)] + A_2 J_{0i}(b) + A_3 J_{3i}(b) \right. \\ \left. + A_4 J_{5i}(b) + A_5 J_{0i}(r_0) + A_6 J_{3i}(r_0) + A_7 J_{\alpha i}(r_0) + A_8 J_{\beta i}(r_0) \right\}, \quad (36)$$

and the dimensionless constants  $A_n$  (independent of  $\sigma$ ,  $Q$ , and  $v$ ) for the Happel and Kuwabara models are given by Eqs. (A9)-(A17) and (A56)-(A64), respectively, in the Appendix. Equations (35) and (36) show that the electrophoretic velocity  $U$  obtained

from using the Neumann condition in Eq. (12b) is always greater than its corresponding result obtained from using the Dirichlet condition in Eq. (12a) by a factor  $(1 + \varphi r_0^3 / 2a^3) / (1 - \varphi r_0^3 / a^3)$  (which increases monotonically with  $\varphi r_0^3 / a^3$  from unity at  $\varphi = 0$  or  $r_0 = 0$ ) under otherwise the same circumstances.

Evidently,  $U_1$  and  $U_2$  in Eq. (35), which are positive, can be deemed as the normalized electrophoretic mobilities of the soft sphere composed of a charged hard core and an uncharged porous shell ( $Q = 0$ ) and of the soft sphere composed of an uncharged hard core ( $\sigma = 0$ ) and a charged porous shell, respectively. Both normalized electrophoretic mobilities are functions of the radius ratio  $r_0/a$ , electrokinetic radius  $\kappa a$ , and shielding parameter  $\lambda a$  of the soft sphere as well as the particle volume fraction  $\varphi = (a/b)^3$  of the suspension. Because of the system's linearity, the effects of the fixed charge densities of the soft sphere on the particle mobility can be simply superimposed. Note that, in the earlier calculations for the electrophoretic mobility of concentrated suspensions of charged soft spheres using the Kuwabara cell model [22, 23],  $\sigma = 0$  was assumed and the contribution from  $U_1$  was missing.

### 3.2 Electric conductivity

The effective electric conductivity for a suspension of charged soft spheres can be obtained from a volume-average current density, with the expression [17]

$$\Lambda = \Lambda^\infty - \frac{3e}{2bkTE_\infty} \sum_{m=1}^M z_m D_m n_m^\infty \int_0^\pi \left( r \frac{\partial \mu_m}{\partial r} - \mu_m \right)_{r=b} \sin \theta \cos \theta d\theta, \quad (37)$$

where  $D_m$  is the diffusion coefficient of the ionic species  $m$  and

$\Lambda^\infty = e^2 \sum_{m=1}^M z_m^2 D_m n_m^\infty / kT$  is the electric conductivity of the fluid solution with no

particles. The substitution of Eqs. (18)-(20) for the ionic electrochemical potential energy  $\mu_m$  together with Eqs. (7) and (8) into Eq. (37) results in the effective conductivity of the suspension correct to the first orders of the fixed charge densities as a linear superposition,

$$A = A^\infty \left[ 1 - \frac{3r_0^3}{2vb^3} - \frac{\gamma ea}{v\epsilon kT} (X_1\sigma + X_2aQ) \right], \quad (38)$$

where

$$\gamma = \frac{\sum_{m=1}^M z_m^3 D_m n_m^\infty}{\sum_{m=1}^M z_m^2 D_m n_m^\infty}, \quad (39)$$

$$X_i = \frac{F_i(b)}{(\kappa a)^i}, \quad (40)$$

which is independent of the reciprocal permeation length  $\lambda$  and the hydrodynamic boundary conditions (Happel and Kuwabara models) at the virtual boundary of the unit cell. The parameters  $X_1$  and  $X_2$  are both positive (and independent of  $\sigma$  and  $Q$ ), thus the presence of the particle charges reduces the magnitude of the effective conductivity for any volume fraction of particles in the suspension if the product of  $\gamma$  and  $\sigma$  (and  $Q$ ) is positive and increases this magnitude if  $\gamma\sigma < 0$  (and  $\gamma Q < 0$ ). Evidently,  $X_1 = X_2 = 0$  and  $A = A^\infty$  as  $\varphi = (a/b)^3 = 0$ . Equations (38)-(40) also result in a greater effect of particle charges on the effective conductivity for the Neumann condition in Eq. (12b) than for the Dirichlet condition in Eq. (12a).



# Chapter 4

## Results and Discussion



The mean electrophoretic mobility and effective electric conductivity for a given suspension of generally charged soft spheres can be readily calculated via Eqs. (35) and (38), respectively. In this chapter, we first consider the mobility and conductivity for the two particular cases of the soft spheres: hard (impermeable) spheres and porous (permeable) spheres. Results for the general case of soft spheres will then be presented.

### 4.1. Suspension of hard spheres

When there is no permeable layer on the surface of the hard core of the soft sphere, the particle reduces to an impermeable sphere of radius  $a = r_0$  and constant surface charge density  $\sigma$ , the terms  $U_2 a Q$  in Eq. (35) and  $X_2 a Q$  in Eq. (38) are trivial, and the dimensionless mobility parameter  $U_1$  calculated from Eq. (36) and conductivity parameter  $X_1$  calculated from Eq. (40) are functions of the electrokinetic particle radius  $\kappa a$  and the particle volume fraction  $\phi$  ( $= a^3 / b^3$ ). The substitution of Eqs. (7), (19a), and (20) into Eq. (40) leads to

$$X_1 = \frac{e^{\kappa(b+r_0)} r_0^2}{8B\kappa^2 ab^3 \nu} \{ \cosh(\kappa b - \kappa r_0) [(48 + 6\kappa^2 r_0^2 + \kappa^4 r_0^4) \{ \kappa b - \tanh(\kappa b - \kappa r_0) \}] \}$$



$$\begin{aligned}
& + \kappa r_0 (48 - 2\kappa^2 r_0^2 - \kappa^4 r_0^4) \{ \kappa b \tanh(\kappa b - \kappa r_0) - 1 \} \\
& + \frac{1}{2} \kappa^6 r_0^6 \cosh(\kappa b) [(1 + \kappa b) \{ \tanh(\kappa b) - 1 \} \{ E_1(-\kappa b) - E_1(-\kappa r_0) \} \\
& + (1 - \kappa b) \{ \tanh(\kappa b) + 1 \} \{ E_1(\kappa b) - E_1(\kappa r_0) \}] - 16\kappa^3 b^3 + 8\kappa^3 r_0^3 - 2\kappa^5 b^{-1} r_0^6 \}, \quad (41)
\end{aligned}$$

where

$$E_n(x) = \int_1^\infty t^{-n} e^{-xt} dt, \quad (42)$$

which is valid for suspensions of both hard spheres and general soft spheres but depends on the boundary condition for  $\psi_a$  at the outer surface of the unit cell given by Eq. (12a) or (12b).

For a suspension of hard spheres with thin electric double layers ( $\kappa a \gg 1$ ), Eqs. (36)

and (41) have the asymptotic forms

$$U_1 \rightarrow \frac{3}{\kappa a} \left( \frac{1 - \varphi^{5/3}}{3 + 2\varphi^{5/3}} - \frac{1}{\kappa a} \right) \quad (43a)$$

for the Happel model in Eq. (25b),

$$U_1 \rightarrow \frac{1}{\kappa a} \left[ 1 - \varphi - \frac{1}{\kappa a} (3 + \varphi^{1/3} - \varphi^{4/3}) \right] \quad (43b)$$

for the Kuwabara model in Eq. (25c), and

$$X_1 \rightarrow \frac{9\varphi}{2(\kappa a)^2 \nu} \left( 1 - \frac{1 + \varphi^{1/3}}{\kappa a} \right) \quad (44)$$

for both models. Note that Eqs. (43) and (44) predict a vanishing particle velocity and no contribution of the particle charges to the effective conductivity in the limit  $\kappa a \rightarrow \infty$  for a constant surface charge density.

For a suspension of hard spheres with thick double layers ( $\kappa a \ll 1$ ), Eqs. (36) and



(41) become

$$U_1 \rightarrow \frac{(1 - \varphi^{1/3})^2 (2 + \varphi)(1 + \varphi^{1/3})(2 + \varphi^{1/3} + 2\varphi^{2/3})}{2(1 + \varphi^{1/3} + \varphi^{2/3})(3 + 2\varphi^{5/3})} \quad (45a)$$

for the Happel model,

$$U_1 \rightarrow \frac{(1 - \varphi^{1/3})^2 (2 + \varphi)(5 + 6\varphi^{1/3} + 3\varphi^{2/3} + \varphi)}{15(1 + \varphi^{1/3} + \varphi^{2/3})} \quad (45b)$$

for the Kuwabara model, and

$$X_1 \rightarrow 3 \frac{\varphi^{1/3} (4 - 15\varphi^{2/3} + 10\varphi + 6\varphi^{5/3} - 5\varphi^2)}{40(1 - \varphi)\nu} \quad (46)$$

for both models. Equations (45) and (46) lead to a finite particle velocity and finite contribution of particle charge to the effective conductivity in the limit  $\kappa a = 0$ .

In the limit  $\varphi \rightarrow 0$  (the suspension is infinitely dilute and  $\nu = 1$ ), Eqs. (36) and (41)

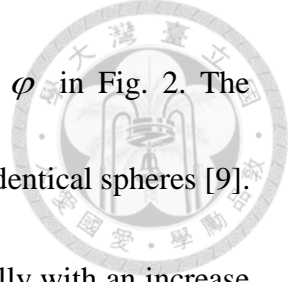
reduce to

$$U_1 \rightarrow \frac{1}{\kappa a + 1} \{1 - e^{\kappa a} [5E_7(\kappa a) - 2E_5(\kappa a)]\}, \quad (47)$$

$$X_1 \rightarrow \frac{\varphi}{16(\kappa a + 1)} [48(\kappa a)^{-2} + 48(\kappa a)^{-1} + 6 - 2\kappa a + (\kappa a)^2 - (\kappa a)^3 + E_1(\kappa a)e^{\kappa a}(\kappa a)^4]. \quad (48)$$

As expected, Eq. (48) indicates that the effect of the particle charges on the electric conductivity of the suspension vanishes in this limit. It can be shown that Eqs. (41)-(48) for the case of constant  $\sigma$  are consistent with the results obtained for the electrophoretic migration and electric conduction of a suspension of hard spheres of constant zeta potential [12].

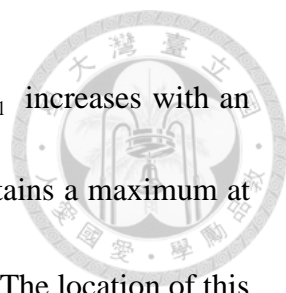
The normalized electrophoretic mobility  $U_1$  for a suspension of hard spheres with constant surface charge density  $\sigma$ , as calculated from Eq. (36) for both the Happel and



Kuwabara cell models, is plotted versus the parameters  $\kappa a$  and  $\varphi$  in Fig. 2. The results are presented up to  $\varphi = 0.74$ , the limit for an assemblage of identical spheres [9].

For a specified value of  $\varphi$ , the value of  $U_1$  decreases monotonically with an increase in  $\kappa a$  (a decrease in the overlap of the adjacent electric double layers) from a constant (equal to  $2/3$  if  $\varphi = 0$ ) at  $\kappa a = 0$  (as predicted from Eq. (45)) to zero as  $\kappa a \rightarrow \infty$  (asymptotically proportional to  $(\kappa a)^{-1}$  as predicted from Eq. (43)). For a fixed value of  $\kappa a$ ,  $U_1$  is a monotonic decreasing function of  $\varphi$  and in general the effect of particle interactions on the electrophoretic mobility is significant. For an arbitrary combination of  $\kappa a$  and  $\varphi$ , the Kuwabara model predicts a smaller value (a stronger particle concentration effect) for the electrophoretic mobility than the Happel model does, but the difference is insubstantial. It can be found that the experimental data of electrophoretic mobility for suspensions of human erythrocytes with large  $\kappa a$  and various values of  $\varphi$  [20] agree well with  $U_1$  predicted from the Happel model with the Dirichlet approach in Eq. (12a) for the suspension of hard spheres.

The parameter  $X_1$  (effect of the particle surface charges) for the effective electric conductivity of a suspension of hard spheres, as calculated from Eq. (41), is plotted versus the parameters  $\kappa a$  and  $\varphi$  in Fig. 3. For a given value of  $\varphi$ , the value of  $X_1$  decreases monotonically with an increase in  $\kappa a$  from a constant at  $\kappa a = 0$  (as predicted from Eq. (46)) to zero as  $\kappa a \rightarrow \infty$  (asymptotically proportional to  $(\kappa a)^{-2}$  as



predicted from Eq. (44)). For a constant value of  $\kappa a$ , however,  $X_1$  increases with an increase in  $\varphi$  from zero at  $\varphi = 0$  (as predicted from Eq. (48)), attains a maximum at some value of  $\varphi$ , and then decreases with a further increase in  $\varphi$ . The location of this maximum shifts to greater  $\varphi$  as  $\kappa a$  increases, and the effect of  $\varphi$  on the effective conductivity can be significant. For specified values of  $\kappa a$  and  $\varphi$ , the value of  $X_1$  obtained from using the Neumann condition in Eq. (12b) is greater than that from using the Dirichlet condition in Eq. (12a). The experimental data of electric conductivity for suspensions of polystyrene latex spheres in aqueous solutions of 0.1 mM HClO<sub>4</sub> with  $\kappa a \approx 1$  and  $\varphi$  of the order 0.01 [19] are in reasonable agreement with  $X_1$  predicted from the Dirichlet approach for the suspension of hard spheres.

## 4.2. Suspension of porous spheres

When the hard core of the soft sphere disappears ( $r_0 = 0$ ), the particle becomes a permeable sphere (such as a polymer coil or colloidal floc) of radius  $a$  and fixed charge density  $Q$ , the terms  $U_1\sigma$  in Eq. (35) and  $X_1\sigma$  in Eq. (38) are trivial, and the mobility parameter  $U_2$  calculated from Eq. (36) and conductivity parameter  $X_2$  calculated from Eq. (40) are functions of the electrokinetic radius  $\kappa a$ , shielding parameter  $\lambda a$ , and particle volume fraction  $\varphi$  and are independent of the boundary condition for  $\psi_a$  at the outer surface of a unit cell given by Eq. (12a) or (12b) ( $\nu = 1$ ). Substitution of Eqs.



(8), (19a), and (20) into Eq. (40) leads to

$$X_2 = \frac{1}{(\kappa a)^2} \left[ \varphi - \frac{\alpha(\kappa a)}{\alpha(\kappa a \varphi^{-1/3})} \right]. \quad (49)$$

For a suspension of porous spheres with thin electric double layers ( $\kappa a \gg 1$ ), Eqs.

(36) and (49) have the forms

$$U_2 \rightarrow \frac{1}{(\lambda a)^2}, \quad (50)$$

$$X_2 \rightarrow \frac{\varphi}{(\kappa a)^2}, \quad (51)$$

for both models. Equations (50) and (51) predict no contribution of particle charges to the effective conductivity but a finite particle velocity in the limit  $\kappa a \rightarrow \infty$ .

For a suspension of porous spheres with thick double layers ( $\kappa a \ll 1$ ), Eqs. (36) and (49) become

$$\begin{aligned} U_2 \rightarrow & \frac{1}{(\lambda a)^2} \left\{ \lambda a [30\varphi^{5/3} + (1 + 14\varphi^{5/3} - 10\varphi^2)(\lambda a)^2 + \frac{1}{3}(2 - 3\varphi^{1/3} + 3\varphi^{5/3} - 2\varphi^2)(\lambda a)^4] \right. \\ & \left. - [30\varphi^{5/3} + (1 + 24\varphi^{5/3} - 10\varphi^2)(\lambda a)^2 - (\varphi^{1/3} - 5\varphi^{5/3} + 4\varphi^2)(\lambda a)^4] \tanh(\lambda a) \right\} \\ & \times \left\{ \lambda a [30\varphi^{5/3} + (3 + 2\varphi^{5/3})(\lambda a)^2] - 3[10\varphi^{5/3} + (1 + 4\varphi^{5/3})(\lambda a)^2] \tanh(\lambda a) \right\}^{-1} \quad (52a) \end{aligned}$$

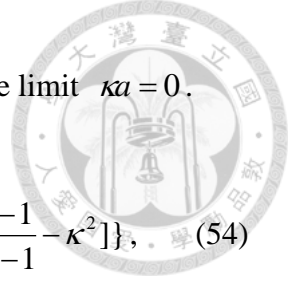
for the Happel model,

$$U_2 \rightarrow \frac{1}{45} \left\{ \frac{15}{(\lambda a)^2} + [1 + 2\varphi(2 - \varphi)] - 6[3\varphi^{1/3} - \varphi(5 - 2\varphi)] + \frac{10(1 - \varphi)^2 \lambda a}{\lambda a - \tanh(\lambda a)} \right\} \quad (52b)$$

for the Kuwabara model, and

$$X_2 \rightarrow \frac{1}{10} (\varphi^{1/3} - \varphi) \quad (53)$$

for both models. Equations (52) and (53) lead to a finite particle velocity and a finite



contribution of the particle charges to the effective conductivity in the limit  $\kappa a = 0$ .

In the limit  $\varphi \rightarrow 0$ , Eqs. (36) and (49) result in

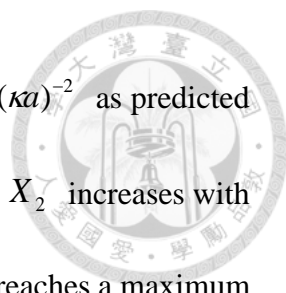
$$U_2 \rightarrow \left(\frac{1}{\lambda a}\right)^2 + \frac{1 - e^{-2\kappa a}}{3(\kappa a)^3} \left\{ \kappa a \coth(\kappa a) - 1 + \frac{\kappa a + 1}{\lambda^2 - \kappa^2} \left[ \lambda^2 \frac{\kappa a \coth(\kappa a) - 1}{\lambda a \coth(\lambda a) - 1} - \kappa^2 \right] \right\}, \quad (54)$$

$$X_2 \rightarrow \frac{\varphi}{(\kappa a)^2}. \quad (55)$$

Again, Eq. (55) predicts no contribution of the particle charges to the effective conductivity in this limit. Equations (49)-(55) are consistent with the results obtained for a suspension of charged porous spheres [17].

In Fig. 4, the normalized electrophoretic mobility  $U_2$  for a suspension of porous spheres, as calculated from Eq. (36) for the Happel cell model (which differs little from that calculated for the Kuwabara model), is plotted as a function of the parameters  $\kappa a$ ,  $\lambda a$ , and  $\varphi$ . For fixed values of  $\lambda a$  and  $\varphi$ , the value of  $U_2$  is a finite monotonic decreasing function of  $\kappa a$  from a constant at  $\kappa a = 0$  (as predicted from Eq. (52)) to another constant as  $\kappa a \rightarrow \infty$  (as predicted from Eq. (50)). For constant values of  $\kappa a$  and  $\varphi$ ,  $U_2$  is a monotonic decreasing function of  $\lambda a$  (the relative resistance to the fluid flow within the porous particle). For given values of  $\kappa a$  and  $\lambda a$ ,  $U_2$  decreases monotonically with an increase in  $\varphi$ ; when  $\kappa a$  is smaller or  $\lambda a$  is greater, the effect of  $\varphi$  on  $U_2$  becomes more conspicuous.

In Fig. 5, the parameter  $X_2$  for the effective electric conductivity of a suspension of porous spheres, as calculated from Eq. (49), is plotted versus the parameters  $\kappa a$  and  $\varphi$ . Analogous to the parameter  $X_1$  for a suspension of hard spheres, the value of  $X_2$  decreases monotonically with an increase in  $\kappa a$  from a constant at  $\kappa a = 0$  (as predicted



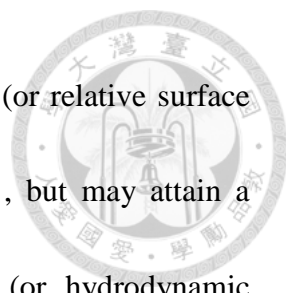
from Eq. (53)) to zero as  $\kappa a \rightarrow \infty$  (asymptotically proportional to  $(\kappa a)^{-2}$  as predicted from Eq. (51)) for a specified value of  $\varphi$ . For a given value of  $\kappa a$ ,  $X_2$  increases with an increase in  $\varphi$  from zero at  $\varphi = 0$  (as predicted from Eq. (55)), reaches a maximum at some value of  $\varphi$  (whose location shifts to greater  $\varphi$  as  $\kappa a$  increases), and then decreases with a further increase in  $\varphi$ . The effect of  $\varphi$  on  $X_2$  can also be significant.

### 4.3. Suspension of soft spheres

For a suspension of soft spheres, the electrophoretic mobility parameters  $U_1$  (contribution from the surface charge density  $\sigma$  of the hard core) and  $U_2$  (contribution from the fixed charge density  $Q$  of the porous surface layer) calculated from Eq. (36) are plotted in Figs. 6 and 7, respectively, for various values of the particle volume fraction  $\varphi$ , radius ratio  $r_0/a$ , electrokinetic radius  $\kappa a$ , and shielding parameter  $\lambda a$ . Analogous to the outcomes of the particular cases with  $r_0/a = 1$  (where  $\lambda a$  is trivial) and  $r_0/a = 0$  discussed in the previous subsections, both mobility parameters in general decrease with an increase in  $\kappa a$  (with some exceptions for  $U_2$ ), decrease with an increase in  $\lambda a$  (from constants at  $\lambda a = 0$  to smaller constants as  $\lambda a \rightarrow \infty$ ), decrease with an increase in  $\varphi$ , and are smaller as predicted by the Kuwabara model than the Happel model (but the difference is insubstantial).

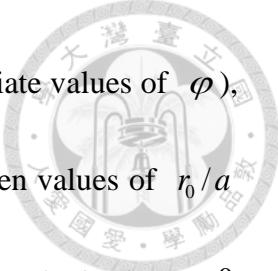
Figure 6b illustrates that, for specified values of  $\kappa a$ ,  $\lambda a$ , and  $\varphi$ , the mobility





parameter  $U_1$  increases with an increase in the radius ratio  $r_0/a$  (or relative surface area of the hard core of the soft particle) from zero at  $r_0/a=0$ , but may attain a maximum and then decrease with a further increase in  $r_0/a$  (or hydrodynamic resistance to the electrophoretic motion of the particle caused by the hard core). On the contrary, as indicated in Fig. 7b, the mobility parameter  $U_2$  is a monotonic decreasing function of  $r_0/a$  (increasing function of  $1-r_0/a$  or the relative volume of the porous surface layer of the soft particle), vanishing at  $r_0/a=1$  as expected. For cases with a medium value of  $r_0/a$  (ca. 1/2), the contributions to the electrophoretic mobility of the soft particle from  $U_1$  and  $U_2$  (or  $\sigma$  and  $Q$ ) are comparable. Our results of  $U_2$  are consistent with the earlier calculations for the electrophoretic mobility of concentrated suspensions of soft spheres with constant  $Q$  and vanishing  $\sigma$  performed by using the Kuwabara cell model [22, 23].

For the effective electric conductivity of a suspension of soft spheres, the parameters  $X_1$  (contribution from the surface charge density  $\sigma$ ) and  $X_2$  (contribution from the fixed charge density  $Q$ ) as calculated from Eq. (40) together with Eq. (19a) (or  $X_1$  as calculated from Eq. (41)) are plotted in Figs. 8 and 9, respectively, for various values of the parameters  $\kappa a$ ,  $r_0/a$ , and  $\varphi$ . Similar to the results of the particular cases with  $r_0/a=1$  and  $r_0/a=0$  discussed in the previous subsections, for constant values of  $\kappa a$  and  $r_0/a$ , both  $X_1$  and  $X_2$  increase with an increase in  $\varphi$  from zero at  $\varphi=0$



but may not be monotonic functions (have maxima at some intermediate values of  $\varphi$ ), and the effect of  $\varphi$  on these parameters can be significant. For given values of  $r_0/a$  and  $\varphi$ , both  $X_1$  and  $X_2$  decrease with an increase in  $\kappa a$  from constants at  $\kappa a = 0$  to zero as  $\kappa a \rightarrow \infty$ . For any combination of  $\kappa a$ ,  $r_0/a$ , and  $\varphi$ , the values of  $X_1$  and  $X_2$  obtained from using the Neumann condition in Eq. (12b) are greater than those from using the Dirichlet condition in Eq. (12a).

For fixed values of  $\kappa a$  and  $\varphi$ , Fig. 8b indicates that the parameter  $X_1$  increases with an increase in the radius ratio  $r_0/a$  from zero at  $r_0/a = 0$ , but may reach a maximum and then decrease with a further increase in  $r_0/a$ . On the contrary, as illustrated in Fig. 9b, the parameter  $X_2$  is a monotonic decreasing function of  $r_0/a$  from a constant at  $r_0/a = 0$  to zero at  $r_0/a = 1$ . For cases with a medium value of  $r_0/a$ , the contributions to the electric conductivity of the suspension from the fixed charge densities  $\sigma$  and  $Q$  of the soft particle are comparable.

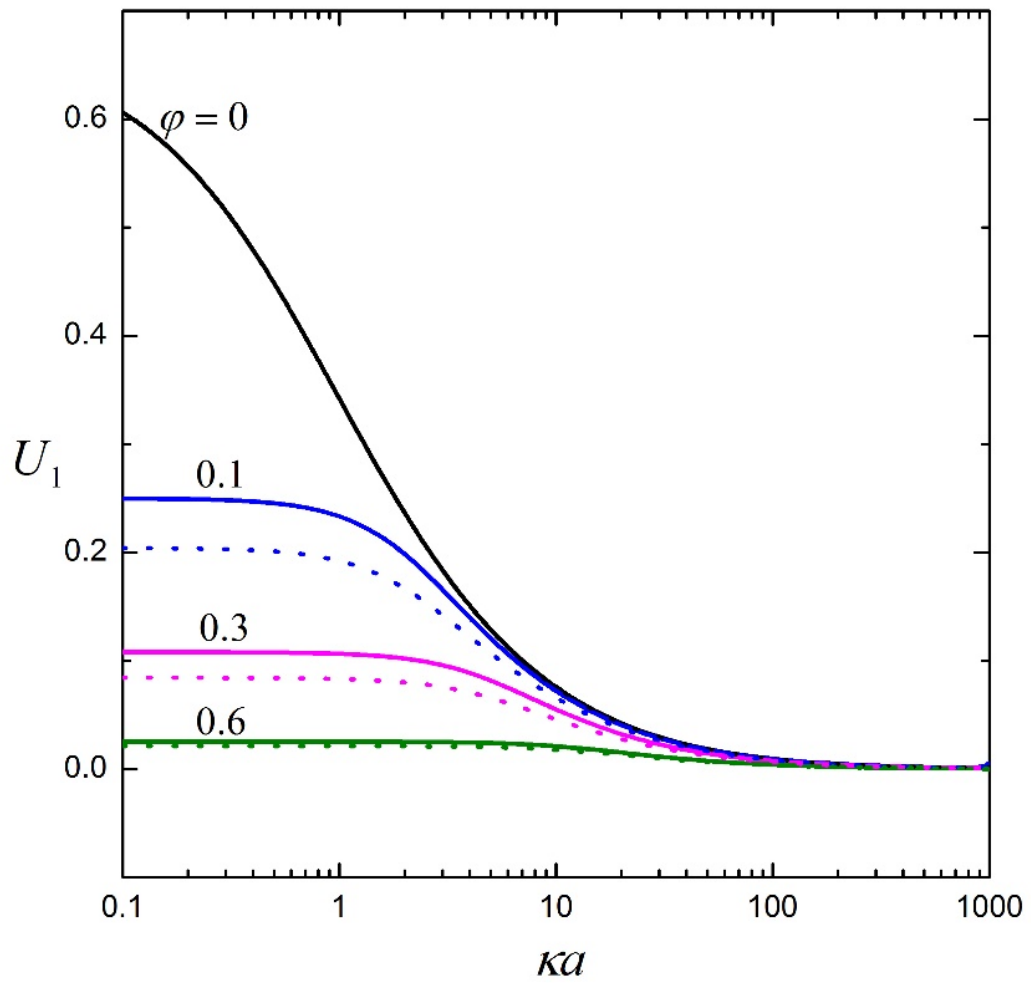


**Figure 2(a).** Plots of the normalized electrophoretic mobility  $U_1$  for a suspension of hard spheres as calculated from Eq. (36) versus the parameter  $\kappa a$ . The solid and dashed curves represent the calculations for the Happel and Kuwabara models, respectively.

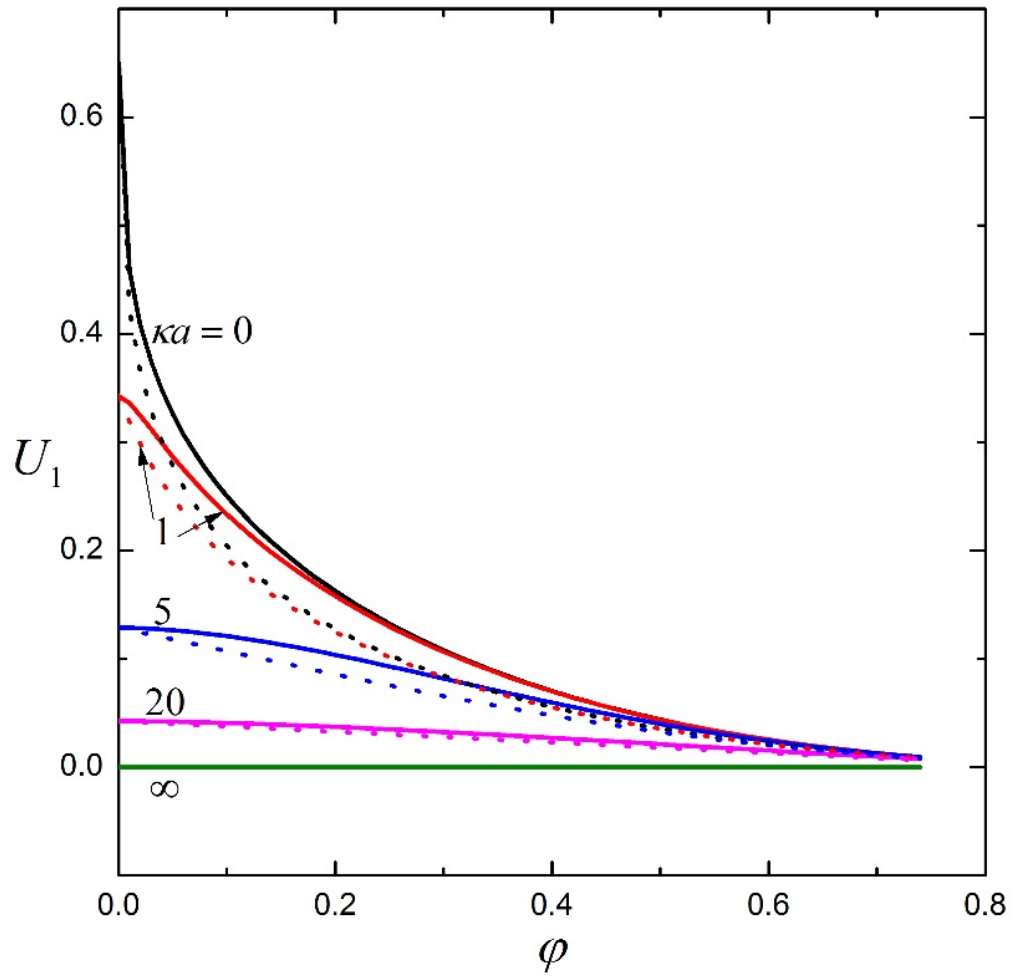


**Figure 2(b).** Plots of the normalized electrophoretic mobility  $U_1$  for a suspension of hard spheres as calculated from Eq. (36) versus the parameter  $\phi$ . The solid and dashed curves represent the calculations for the Happel and Kuwabara models, respectively.

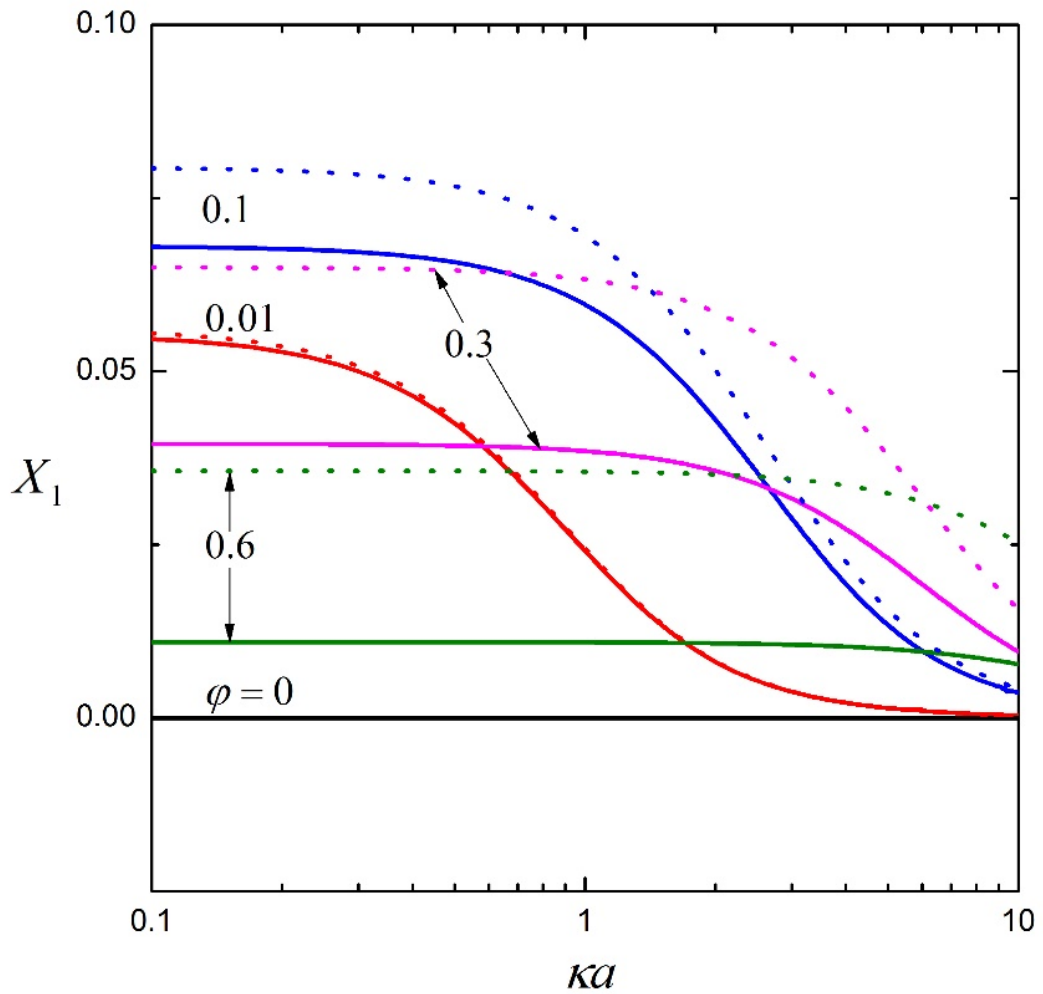


**Figure 3(a).** Plots of the electric conductivity parameter  $X_1$  for a suspension of hard spheres as calculated from Eq. (41) versus the parameter  $\kappa a$ . The solid and dashed curves represent the calculations from using the Dirichlet condition in Eq. (12a) and Neumann condition in Eq. (12b), respectively.

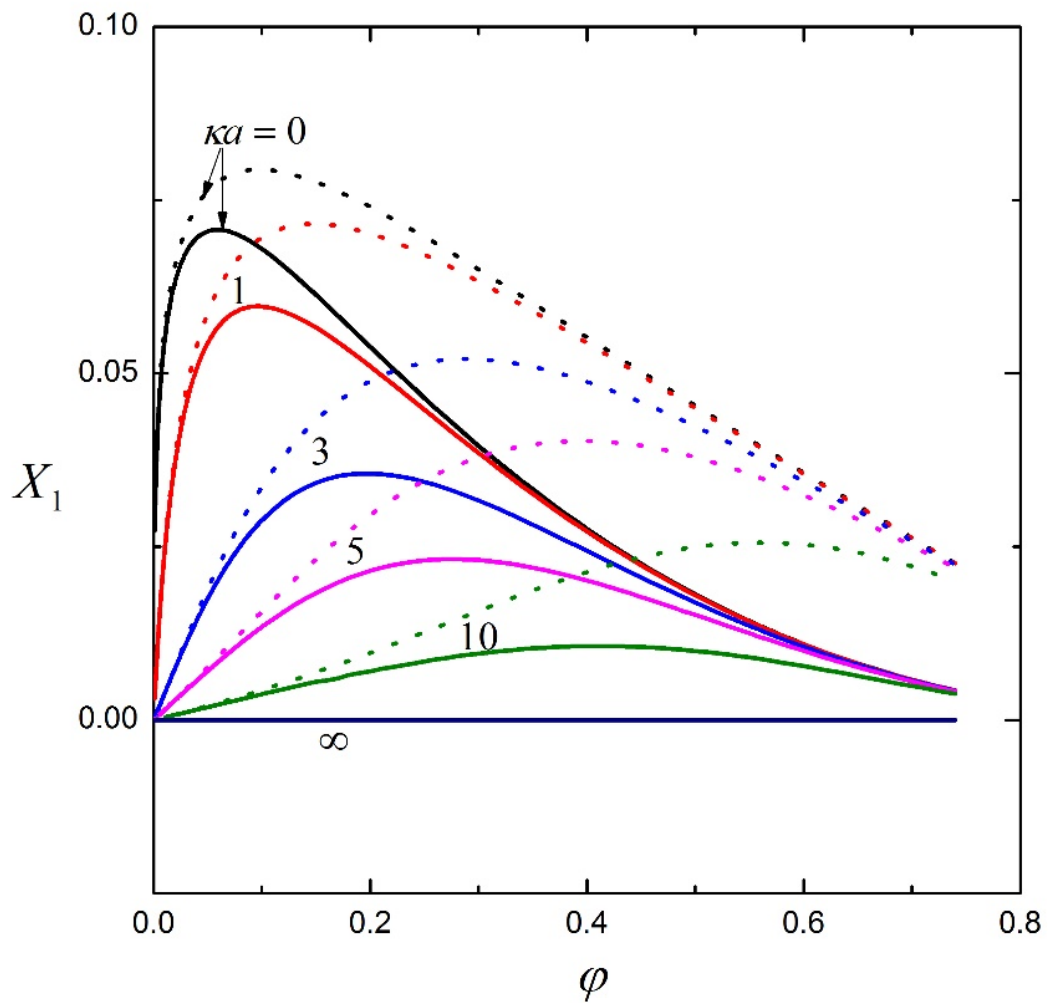


**Figure 3(b).** Plots of the electric conductivity parameter  $X_1$  for a suspension of hard spheres as calculated from Eq. (41) versus the parameter  $\varphi$ . The solid and dashed curves represent the calculations from using the Dirichlet condition in Eq. (12a) and Neumann condition in Eq. (12b), respectively.

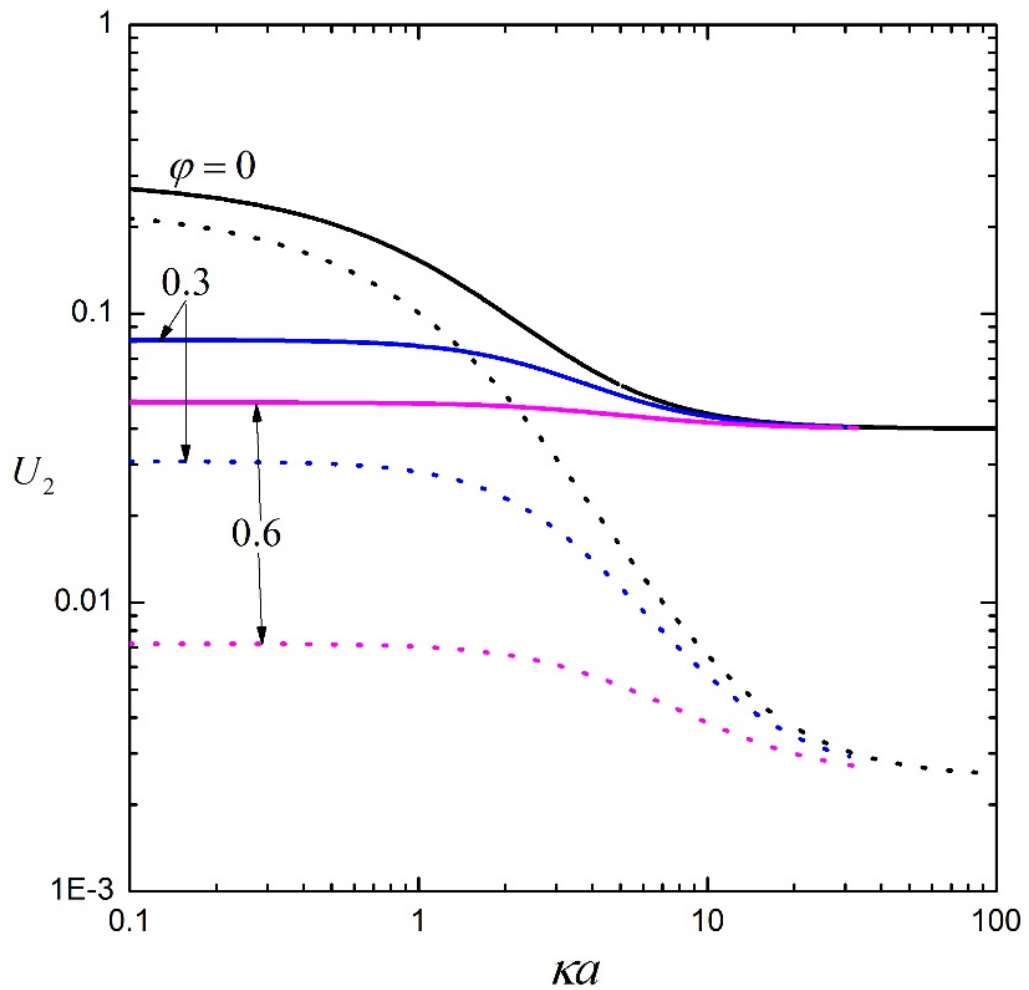


**Figure 4(a).** Plots of the normalized electrophoretic mobility  $U_2$  for a suspension of porous spheres as calculated from Eq. (36) versus the parameter  $\kappa a$  for the Happel model. The solid and dashed curves represent the calculations with  $\lambda a = 5$  and  $\lambda a = 20$ , respectively.

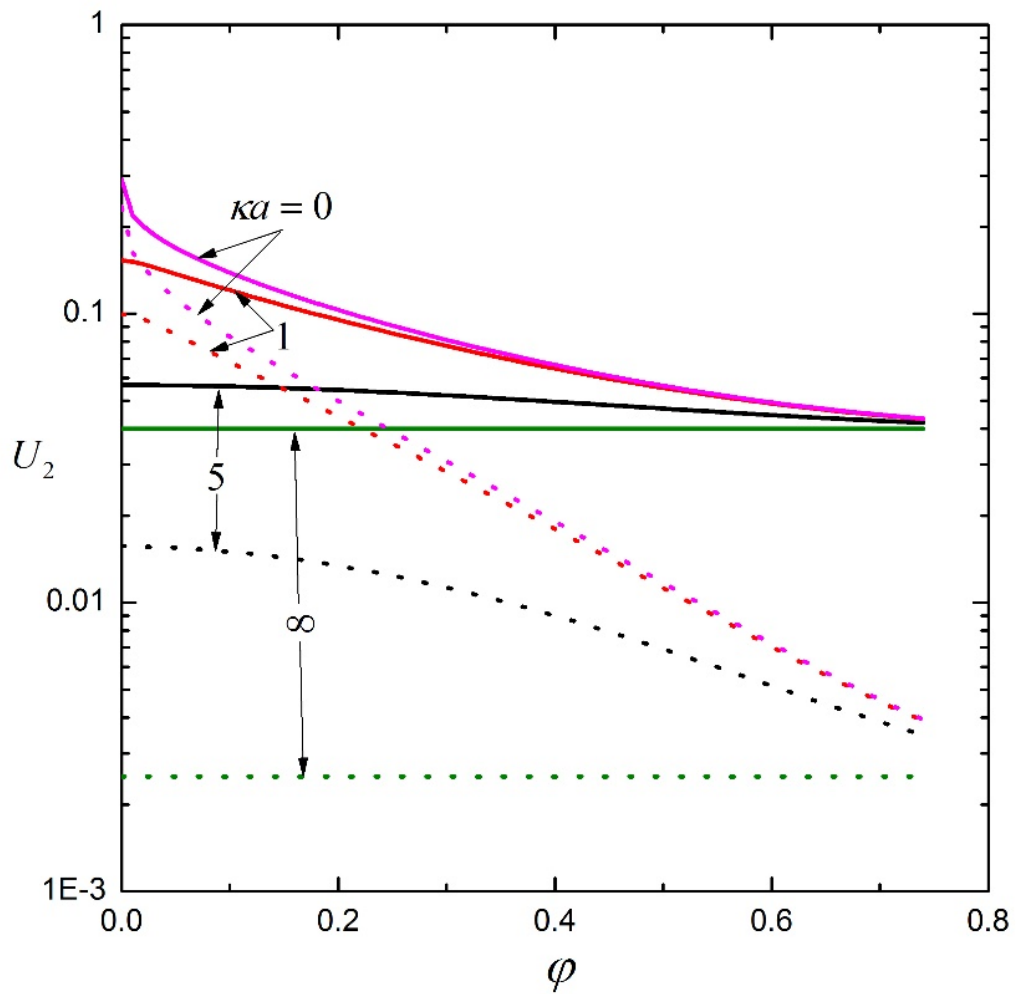


**Figure 4(b).** Plots of the normalized electrophoretic mobility  $U_2$  for a suspension of porous spheres as calculated from Eq. (36) versus the parameter  $\varphi$  for the Happel model. The solid and dashed curves represent the calculations with  $\lambda a = 5$  and  $\lambda a = 20$ , respectively.



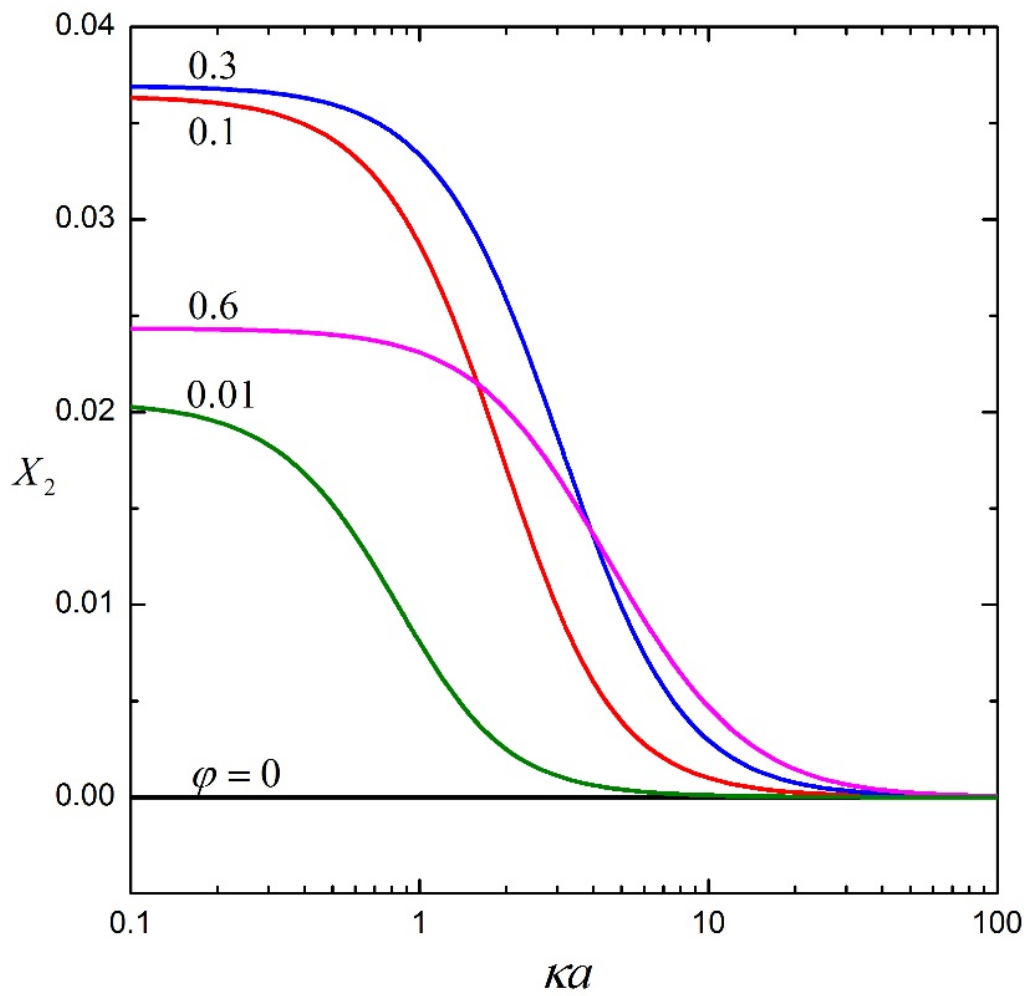


**Figure 5(a).** Plots of the electric conductivity parameter  $X_2$  for a suspension of porous spheres as calculated from Eq. (49) versus the parameter  $\kappa a$  .

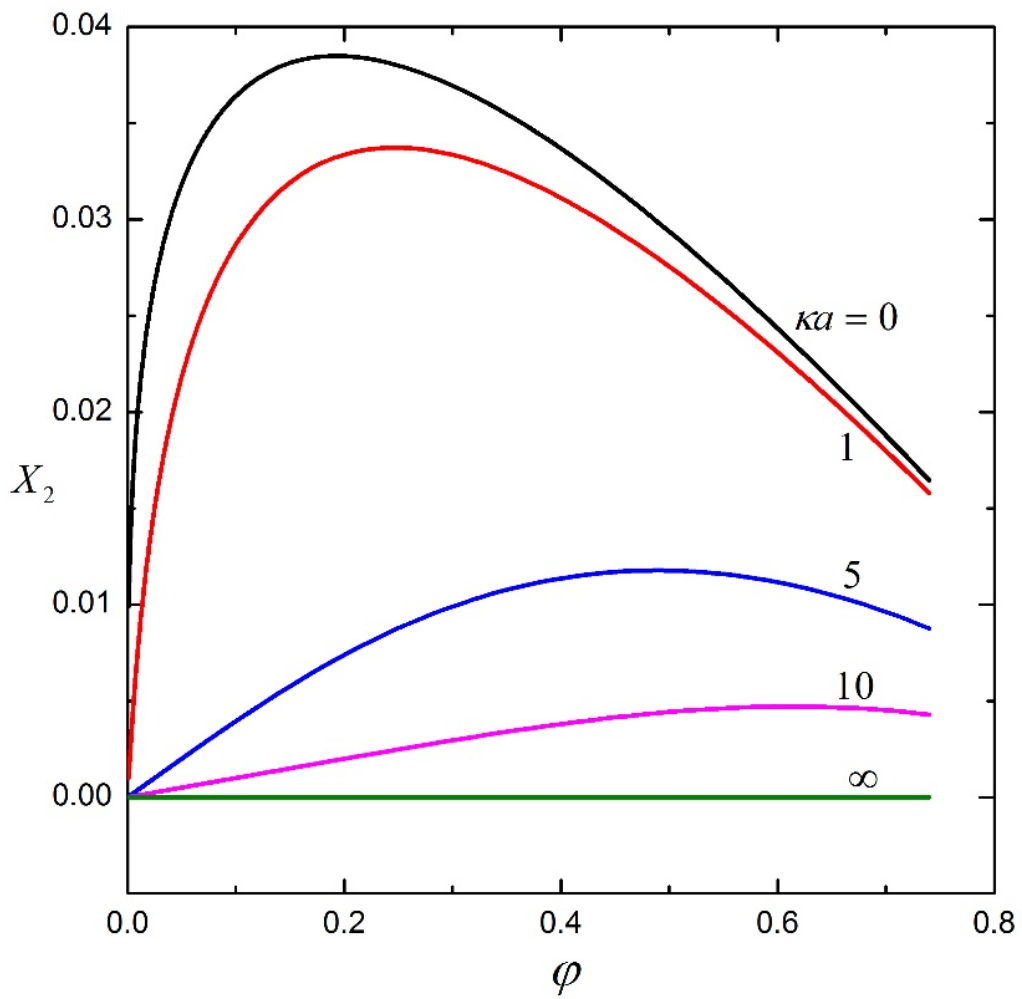


**Figure 5(b).** Plots of the electric conductivity parameter  $X_2$  for a suspension of porous spheres as calculated from Eq. (49) versus the parameter  $\phi$ .

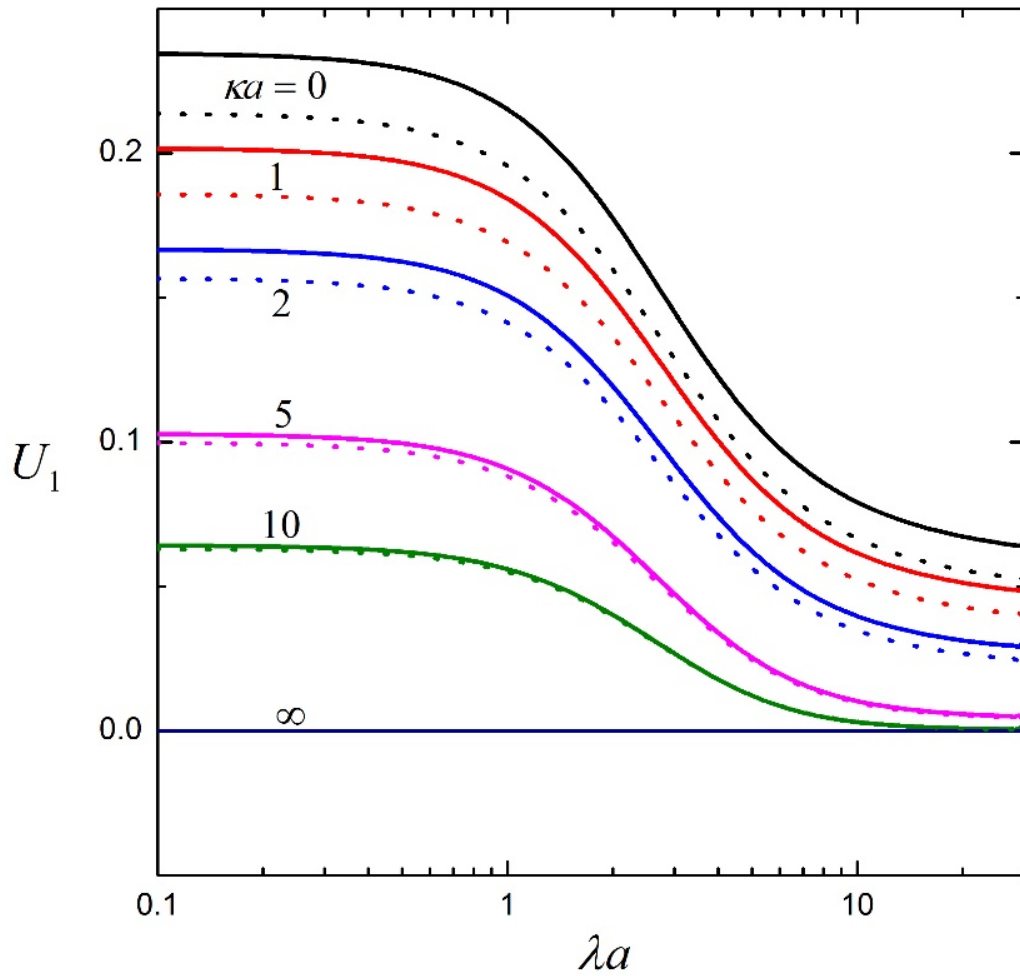


**Figure 6(a).** Plots of the electrophoretic mobility parameter  $U_1$  for a suspension of soft spheres as calculated from Eq. (36) versus the parameter  $\lambda a$  for various values of  $\kappa a$  at  $\varphi = 0.1$  and  $r_0/a = 0.5$ . The solid and dashed curves represent the calculations for the Happel and Kuwabara models, respectively.

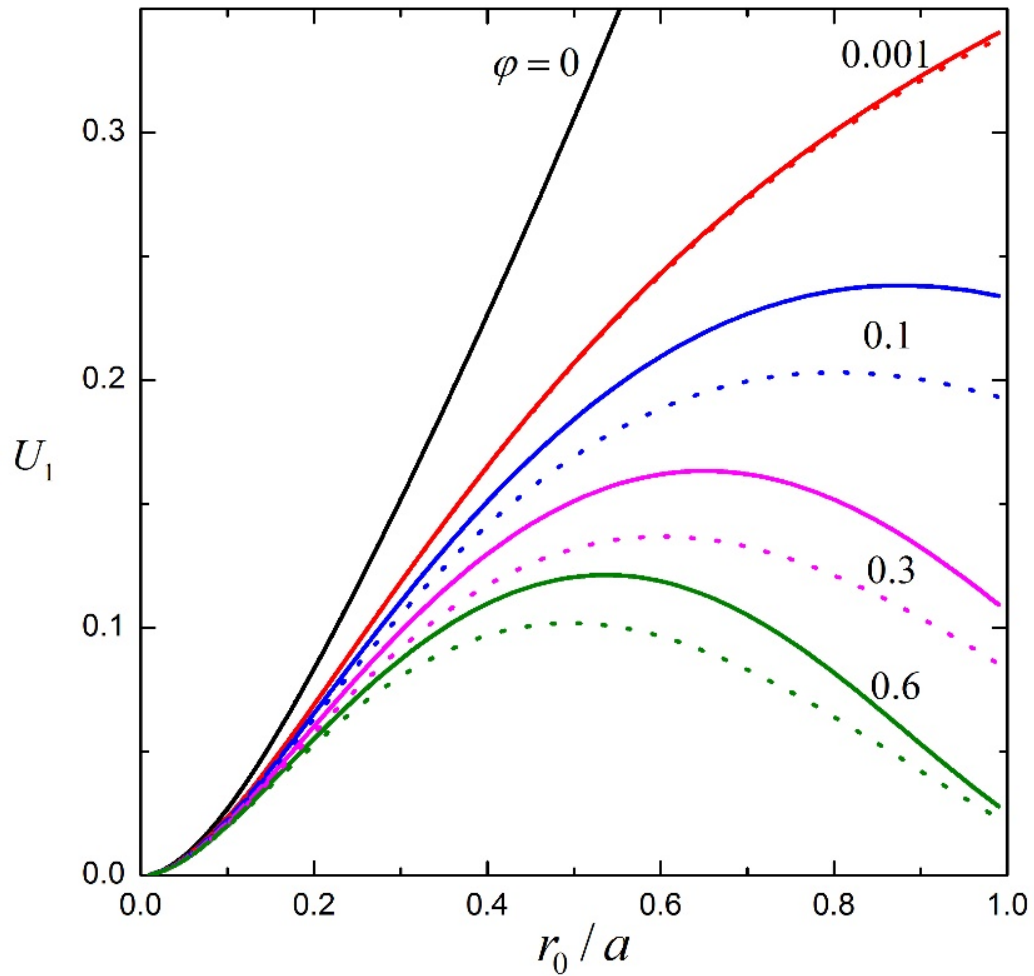


**Figure 6(b).** Plots of the electrophoretic mobility parameter  $U_1$  for a suspension of soft spheres as calculated from Eq. (36) versus the parameter  $r_0/a$  for various values of  $\varphi$  at  $\kappa a = 1$  and  $\lambda a = 1$ . The solid and dashed curves represent the calculations for the Happel and Kuwabara models, respectively.

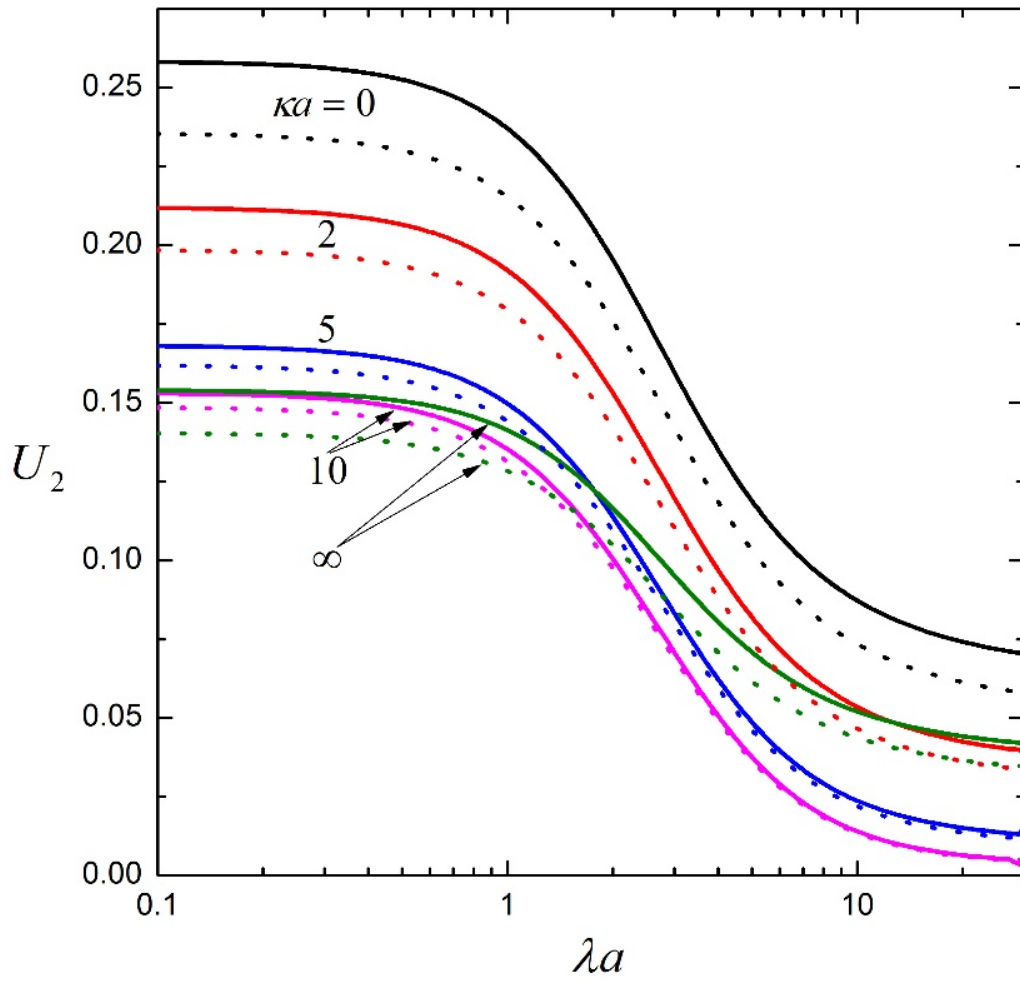


**Figure 7(a).** Plots of the electrophoretic mobility parameter  $U_2$  for a suspension of soft spheres as calculated from Eq (36) versus the parameter  $\lambda a$  for various values of  $\kappa a$  at  $\varphi = 0.1$  and  $r_0/a = 0.5$ . The solid and dashed curves represent the calculations for the Happel and Kuwabara models, respectively.

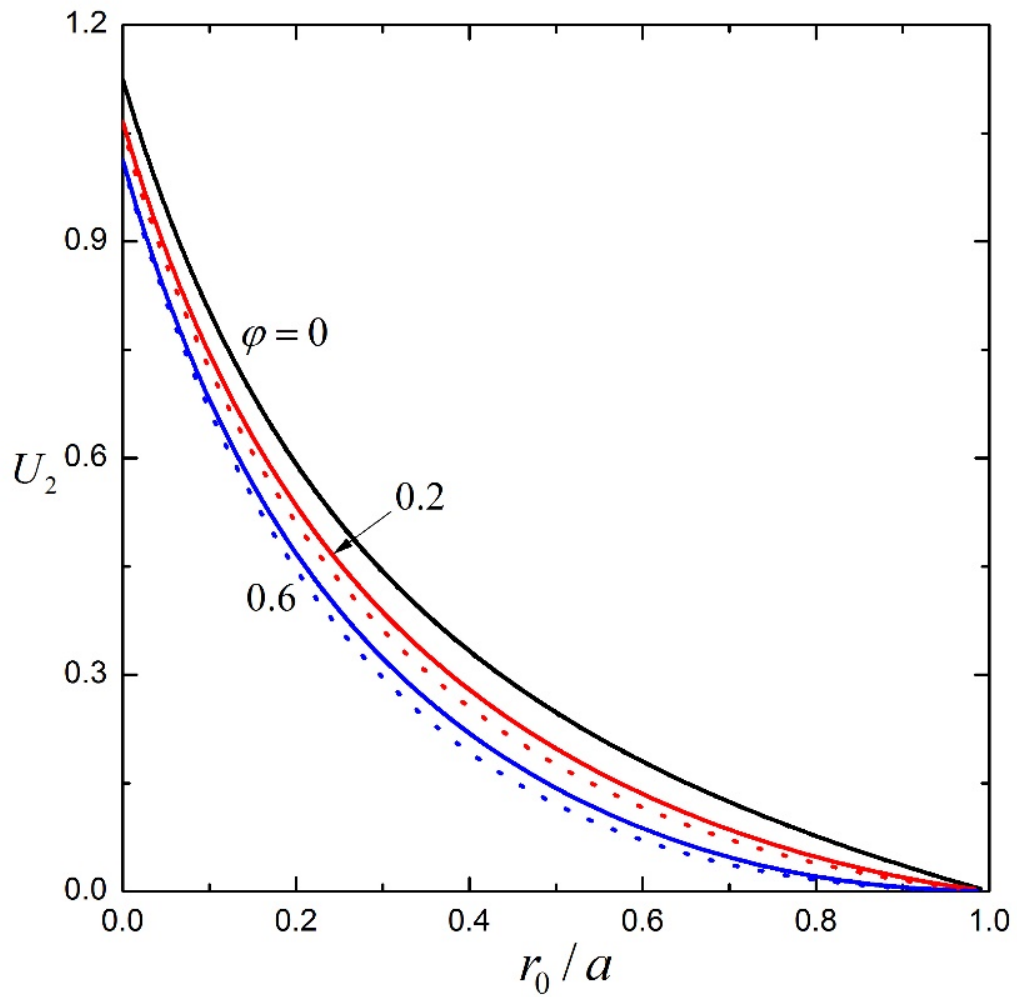


**Figure 7(b).** Plots of the electrophoretic mobility parameter  $U_2$  for a suspension of soft spheres as calculated from Eq (36) versus the parameter  $r_0/a$  for various values of  $\phi$  at  $\kappa a = 1$  and  $\lambda a = 1$ . The solid and dashed curves represent the calculations for the Happel and Kuwabara models, respectively.

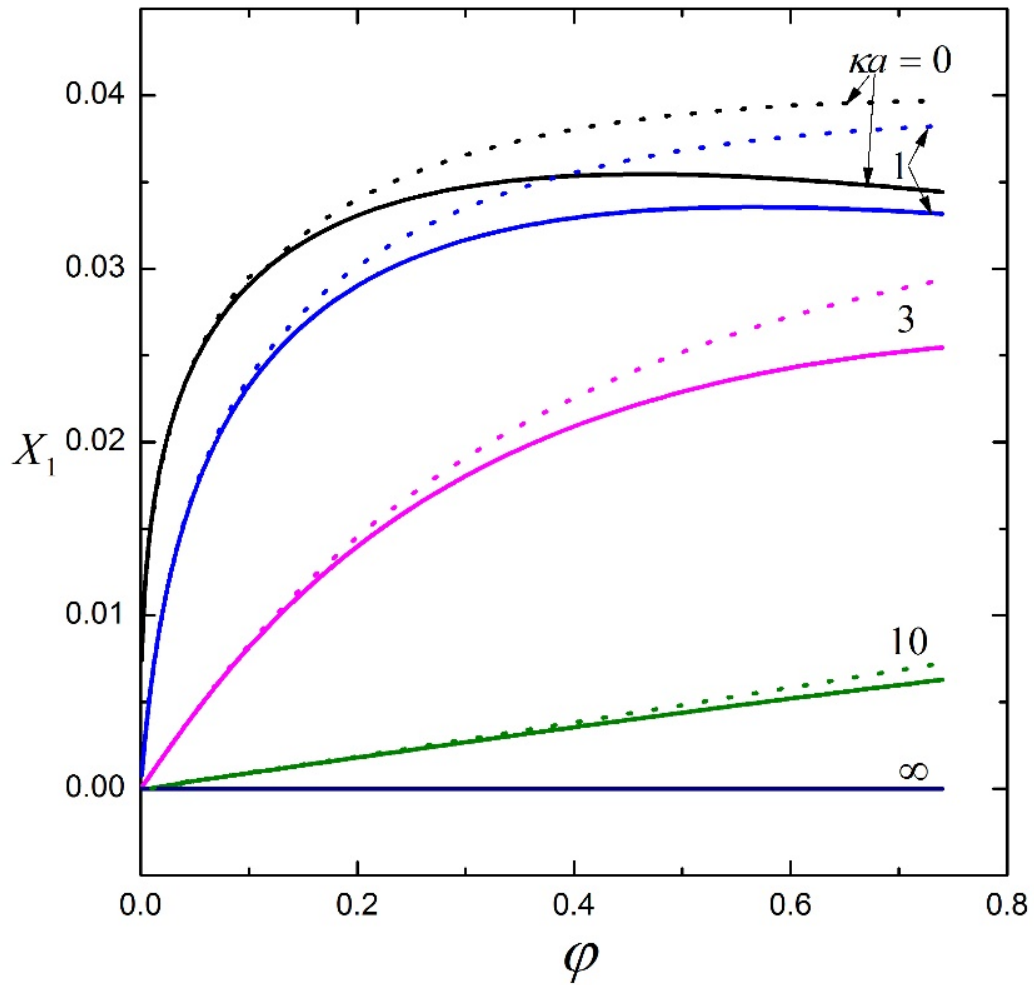


**Figure 8(a).** Plots of the electric conductivity parameter  $X_1$  for a suspension of soft spheres as calculated from Eq. (40) or (41) versus the parameter  $\varphi$  for various values of  $\kappa a$  at  $r_0/a = 0.5$ . The solid and dashed curves represent the calculations from using the Dirichlet condition in Eq. (12a) and Neumann condition in Eq. (12b), respectively.

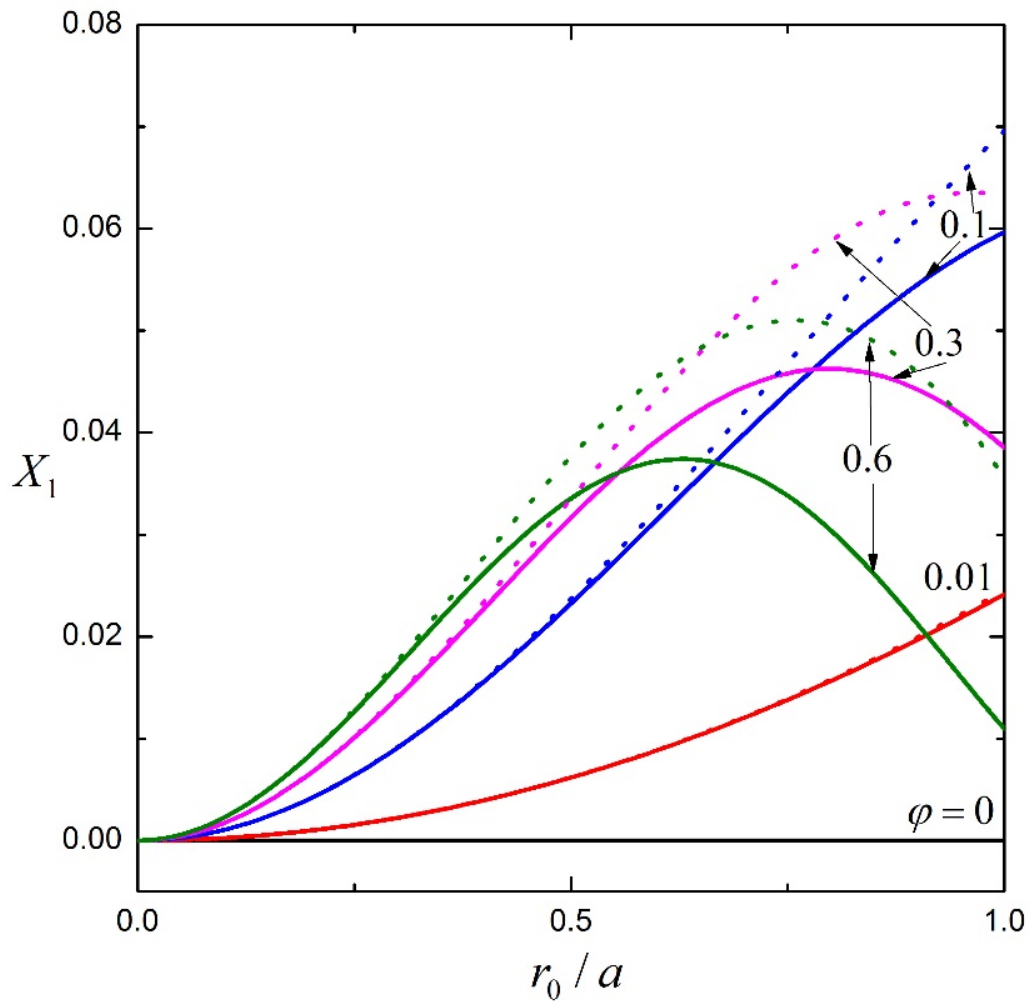


**Figure 8(b).** Plots of the electric conductivity parameter  $X_1$  for a suspension of soft spheres as calculated from Eq. (40) or (41) versus the parameter  $r_0/a$  for various values of  $\varphi$  at  $\kappa a = 1$ . The solid and dashed curves represent the calculations from using the Dirichlet condition in Eq. (12a) and Neumann condition in Eq. (12b), respectively.



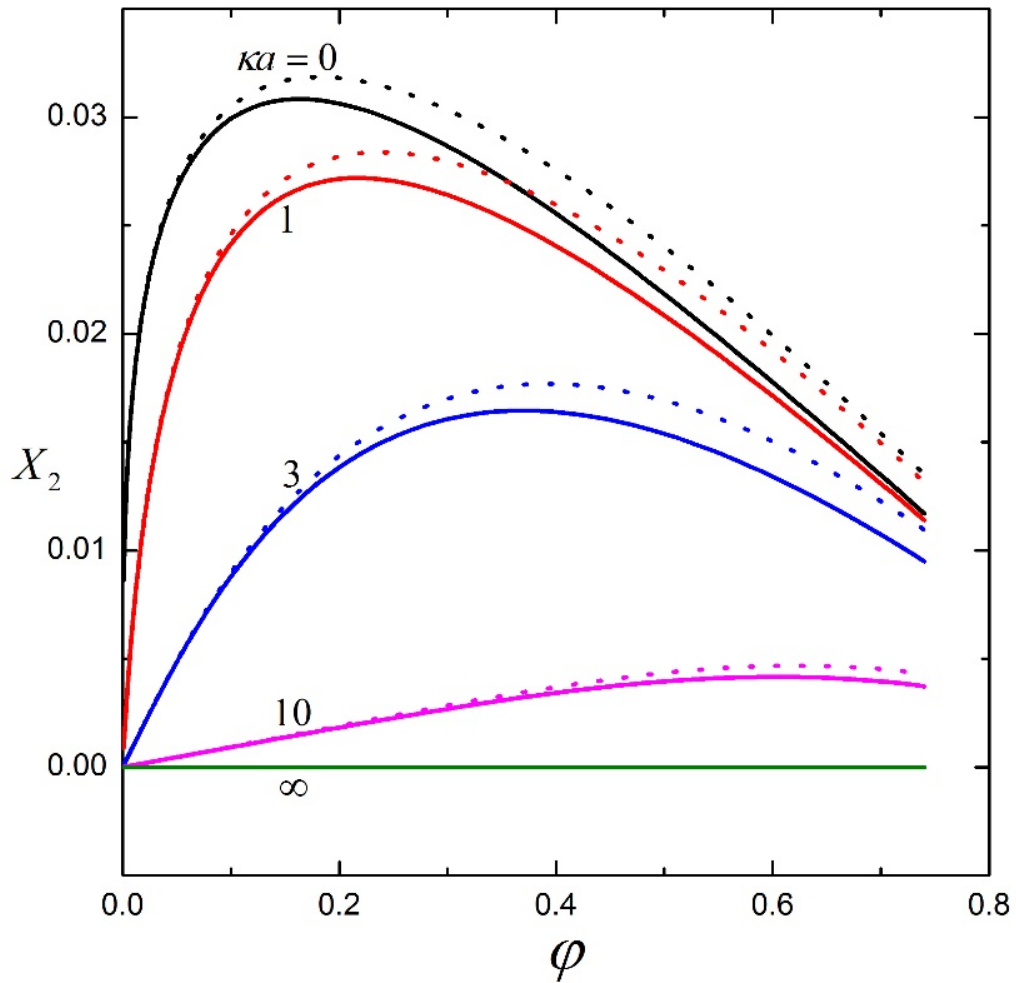


**Figure 9(a).** Plots of the electric conductivity parameter  $X_2$  for a suspension of soft spheres as calculated from Eq. (40) versus the parameter  $\varphi$  for various values of  $\kappa a$  at  $r_0/a = 0.5$ . The solid and dashed curves represent the calculations from using the Dirichlet condition in Eq. (12a) and Neumann condition in Eq. (12b), respectively.

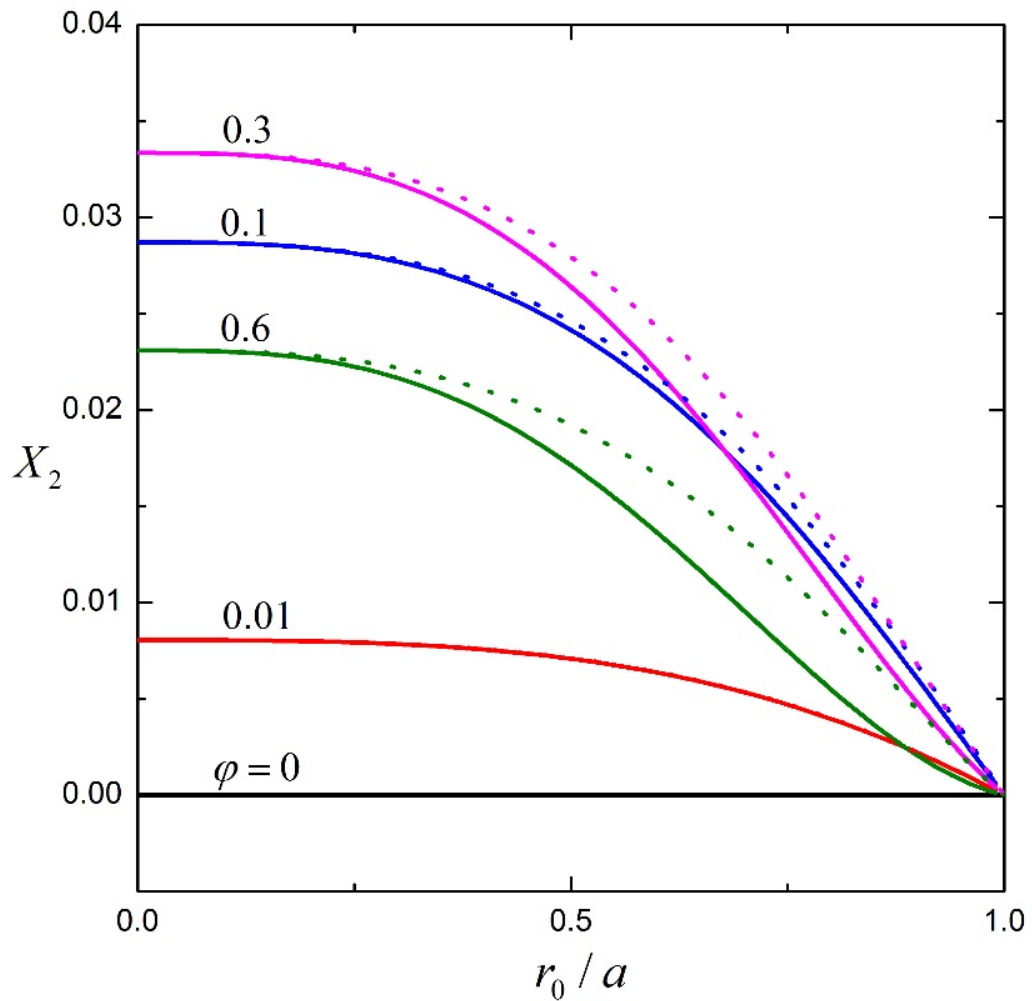


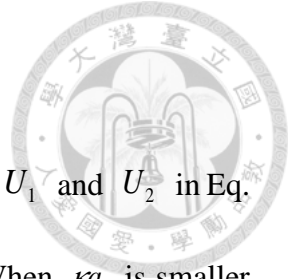
**Figure 9(b).** Plots of the electric conductivity parameter  $X_2$  for a suspension of soft spheres as calculated from Eq. (40) versus the parameter  $r_0/a$  for various values of  $\phi$  at  $\kappa a = 1$ . The solid and dashed curves represent the calculations from using the Dirichlet condition in Eq. (12a) and Neumann condition in Eq. (12b), respectively.

# Chapter 5

## Concluding Remarks



Using a unit cell model, we analyze the electrophoresis and electric conduction in a suspension of charged soft particles thoroughly in this thesis. Each soft sphere is a hard core of radius  $r_0$  and surface charge density  $\sigma$  covered with a permeable porous layer of thickness  $a - r_0$  in which frictional segments with fixed charge density  $Q$  distribute uniformly. The equilibrium electric potential profile outside the hard core in a unit cell and its perturbation caused by the applied electric field are obtained from solving the linearized Poisson-Boltzmann and Laplace equations, respectively. The ionic electrochemical potential energy and fluid flow fields are then obtained by solving the ionic continuity equation and modified Stokes/Brinkman equation, respectively. Through the use of a force balance and a volume-average current density, explicit formulas for the electrophoretic mobility of the soft spheres and effective electric conductivity of the suspension as linear functions of the fixed charge densities  $\sigma$  and  $Q$  are obtained in Eqs. (35) and (38) for arbitrary values of the radius ratio  $r_0/a$ , electrokinetic radius  $\kappa a$ , and shielding parameter  $\lambda a$  of the soft spheres as well as the particle volume fraction  $\varphi$  of the suspension. In the limits  $r_0 = a$  and  $r_0 = 0$ , these formulas for a suspension of charged soft spheres reduce to the corresponding formulas of charged hard spheres and



charged porous spheres, respectively.

Our results indicate that the electrophoretic mobility parameters  $U_1$  and  $U_2$  in Eq. (35) in general decrease with increases in  $\kappa a$ , in  $\lambda a$ , and in  $\varphi$ . When  $\kappa a$  is smaller or  $\lambda a$  is greater, the effect of  $\varphi$  on the mobility parameters becomes more substantial. On the other hand, the effects of particle charges on the effective electric conductivity or the parameters  $X_1$  and  $X_2$  in Eq. (38) decrease with an increase in  $\kappa a$  from constants at  $\kappa a = 0$  to zero as  $\kappa a \rightarrow \infty$  and increase with an increase in  $\varphi$  from zero at  $\varphi = 0$  but may not be monotonic functions (have maxima at some intermediate values of  $\varphi$ ). When  $\kappa a$  is smaller, the effect of  $\varphi$  on  $X_1$  and  $X_2$  is also more conspicuous. In general, the effects of  $r_0/a$ ,  $\kappa a$ ,  $\lambda a$ , and  $\varphi$  on the electrophoretic mobility and effective electric conductivity are interesting, significant, and complicated. These results provide valuable information for interpreting experimental data.

Equations (35) and (38) show that the effects of particle charges on the electrophoretic mobility of the soft particles and effective electric conductivity of the suspension obtained from the unit cell model using the Neumann condition in Eq. (12b) is always greater than their corresponding results obtained from using the Dirichlet condition in Eq. (12a) under otherwise the same circumstances. Also, the Kuwabara cell model predicts a smaller value (a stronger particle concentration effect) for the electrophoretic mobility than the Happel model does, but the difference is insubstantial.

# Lists of Symbols



$a$	the radius of the soft sphere, m
$b$	the radius of the unit cell, m
$B$	defined by Eq. (9)
$D_m$	diffusion coefficient of the species $m$ , $\text{m}^2 \cdot \text{s}^{-1}$
$e$	the elementary electric charge, C
$\mathbf{e}_r$	the unit normal vector outward from the composite sphere surface
$\mathbf{e}_z$	the unit vector in the z-direction
$E_n(x)$	defined by Eq. (42)
$E_\infty$	the magnitude of applied electric field, $\text{V} \cdot \text{m}^{-1}$
$F_i(r)$	the dimensionless functions of $r$ given by Eq. (19)
$\mathbf{F}_e$	the electric force acting on the soft sphere, N
$\mathbf{F}_h$	the hydrodynamic drag force acting on the soft sphere, N
$h(r)$	unit step function
$I_{ni}(r_1, r_2)$	defined by Eq. (20)
$J_{\alpha i}(r)$	defined by Eq. (31a)
$J_{\beta i}(r)$	defined by Eq. (31b)
$J_{ni}(r)$	defined by Eq. (31c)



$k$	Boltzmann's constant, $\text{J} \cdot \text{K}^{-1}$
$n_m^\infty$	the bulk concentration of species $m$ , $\text{m}^{-3}$
$p$	the pressure distribution, $\text{N} \cdot \text{m}^{-2}$
$Q$	the volumetric fixed-charge density of the porous layer, $\text{C} \cdot \text{m}^{-3}$
$r_0$	the radius of the rigid core, $\text{m}$
$r, \theta, \phi$	spherical coordinates
$T$	the absolute temperature, $\text{K}$
$\mathbf{u}$	the fluid velocity distribution, $\text{m} \cdot \text{s}^{-1}$
$u_r, u_\theta$	$r$ and $\theta$ components, respectively, of $\mathbf{u}$ , $\text{m} \cdot \text{s}^{-1}$
$U$	the electrophoretic velocity of the particle, $\text{m} \cdot \text{s}^{-1}$
$U_i$	the electrophoretic mobility parameters defined by Eq. (35)
$X_i$	defined by Eq. (40)
$z_m$	the valence of species $m$

### Greeks

$\rho$	the space charge density in the fluid phase, $\text{C} \cdot \text{m}^{-3}$
$\varepsilon$	the dielectric permittivity of the electrolyte solution, $\text{C}^2 \cdot \text{J}^{-1} \cdot \text{m}^{-1}$
$\varphi$	the particle volume fraction
$\alpha(x)$	defined by Eq. (32a)

$\beta(x)$	defined by Eq. (32b)
$\eta$	the viscosity of the fluid, $\text{kg} \cdot \text{m}^{-1} \cdot \text{s}^{-1}$
$\kappa$	reciprocal of the Debye screening length, $\text{m}^{-1}$
$\lambda$	the reciprocal of a constant shielding length featuring the extent of flow penetration inside the porous layer, $\text{m}^{-1}$
$\mu_m$	the electrochemical potential energy distribution of species $m$ , J
$\psi$	the electric potential distribution, V
$\psi_{\text{eq}}$	the equilibrium electric potential distribution, V
$\psi_a$	the small perturbation to the equilibrium state of electric potential distribution, V
$\tau_{rr}, \tau_{r\theta}$	the non-vanishing components of the viscous stress of the fluid,  $\text{N} \cdot \text{m}^{-2}$
$\gamma$	defined by Eq. (39)
$\Lambda$	the effective electric conductivity of the suspension,  $\text{C}^2 \cdot \text{m}^{-1} \cdot \text{s}^{-1} \cdot \text{J}^{-1}$



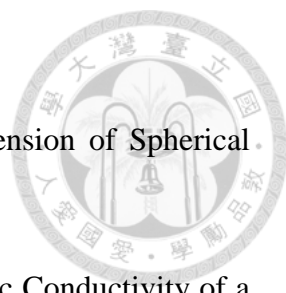
## References



- (1) Dukhin, S.S.; Derjaguin, B.V. Electrokinetic Phenomena. *Surface and Colloid Science*; Matijevic, E., Ed.; Wiley: New York **1974**; Vol. 7, 1-351.
- (2) Saville, D.A. Electrical Conductivity of Suspensions of Charged Particles in Ionic Solutions. *J. Colloid Interface Sci.* **1979**, 71:477-490.
- (3) O'Brien, R.W. The Electrical Conductivity of a Dilute Suspension of Charged Particles. *J. Colloid Interface Sci.* **1981**, 81:234-248.
- (4) Ohshima, H.; Healy, T. W.; White, L. R. Approximate Analytic Expressions for the Electrophoretic Mobility of Spherical Colloidal Particles and the Conductivity of their Dilute Suspensions. *J. Chem. Soc., Faraday Trans. 2.* **1983**, 79, 1613– 1628.
- (5) Hermans, J. J.; Fujita, H. Electrophoresis of a Charged Polymer Molecules with Partial Free Drainage. *Proc. K. Ned. Akad. Wet., Ser. B: Palaeontol., Geol., Phys., Chem.* **1955**, 58, 182– 187.
- (6) Liu, Y. C.; Keh, H. J. The Electric Conductivity of Dilute Suspensions of Charged Porous Spheres. *J. Colloid Interface Sci.* **1997**, 192, 375-385.
- (7) Ohshima, H. Electrophoretic Mobility of Soft Particles. *J. Colloid Interface Sci.* **1994**, 163, 474-483.
- (8) Liu, Y. C.; Keh, H. J. Electric Conductivity of a Dilute Suspension of Charged Composite Spheres. *Langmuir* **1998**, 14, 1560-1574.
- (9) Levine, S.; Neale, G.H. The Prediction of Electrokinetic Phenomena within Multiparticle Systems I. Electrophoresis and Electroosmosis, *J. Colloid Interface Sci.* **1974**, 47:520-529.
- (10) Zharkikh, N. I.; Shilov, V. N. Theory of Collective Electrophoresis of Spherical Particles in the Henry Approximation. *Colloid J. USSR (English translation)* **1982**,



43, 865-870.

- 
- (11) Ohshima, H. Electrical Conductivity of a Concentrated Suspension of Spherical Colloidal Particles. *J. Colloid Interface Sci.* **1999**,212, 443–448.
- (12) Ding, J.M.; Keh, H.J. The Electrophoretic Mobility and Electric Conductivity of a Concentrated Suspension of Colloidal Spheres with Arbitrary Double-Layer Thickness. *J. Colloid Interface Sci.* **2001**,236:180-193.
- (13) Keh, H.J.; Ding J.M. Electrophoretic Mobility and Electric Conductivity of Suspensions of Charge-Regulating Colloidal Spheres. *Langmuir* **2002**,18:4572-4583
- (14) Carrique, F.; Cuquejo, J.; Arroyo, F. J.; Jiménez, A. V.; Delgado, M. L. Influence of Cellmodel Boundary Conditions on the Conductivity and Electrophoretic Mobility of Concentrated Suspensions. *Adv. Colloid Interface Sci.* **2005**,118, 43–50.
- (15) Cuquejo, J.; Jimenez, M.L.; Delgado, A.V.; et al. Numerical and Analytical Studies of the Electrical Conductivity of a Concentrated Colloidal Suspension. *J. Phys. Chem. B.* **2006**,110, 6179–6189.
- (16) Zholkovskiy<sup>1</sup>, E.K.; Masliyah, J.H.; Shilov, V.N.; Bhattacharjee, S. Electrokinetic Phenomena in Concentrated Disperse Systems: General Problem Formulation and Spherical Cell Approach. *Adv. Colloid Interface Sci.* **2007**, 134-135:279-321.
- (17) Keh, H.J.; Liu, C.P. Electric Conductivity and Electrophoretic Mobility in Suspensions of Charged Porous Spheres. *J. Phys. Chem. C.* **2010**, 114:22044-22054.
- (18) Huang, H.Y.; Keh, H.J. Electrophoretic Mobility and Electric Conductivity in Suspensions of Charge-Regulating Porous Particles. *Colloid Polym. Sci.* **2015**, 293:1903-1914.
- (19) Watillon A.; Stone-Masui, J. Surface Conductance in Dispersions of Spherical Particles Study of Monodisperse Polystyrene Lattices. *J. Electroanal Chem.* **1972**,37:143-160.

- 
- (20) Zukoski, C.F.; Saville, D.A. Electrokinetic Properties of Particles in Concentrated Suspensions. *J. Colloid Interface Sci.* **1987**, 115:422-436.
- (21) Miller, N.P.; Berg, J.C. Experiments on the Electrophoresis of Porous Aggregates. *J. Colloid Interface Sci.* **1993**, 159:253-254.
- (22) Ohshima, H. Electrophoretic Mobility of Soft Particles in Concentrated Suspensions. *J. Colloid Interface Sci.* **2000**, 225:233-242.
- (23) Lopez-Garcia, J.J.; Grosse, C.; Horno, J. Numerical Calculation of the Electrophoretic Mobility of Concentrated Suspensions of Soft Particles. *J. Colloid Interface Sci.* **2006**,301:651-659.
- (24) Ahualli, S.; Jimenez, M.L.; Carrique, F.; Delgado, A.V. AC Electrokinetics of Concentrated Suspensions of Soft Particles. *Langmuir* **2009**, 25:1986-1997.
- (25) Keh, H. J.; Hsieh, T. H. Electrophoresis of a Colloidal Sphere in a Spherical Cavity with Arbitrary Zeta Potential Distributions. *Langmuir* **2007**, 23:7928-7935.
- (26) Chen, W.J.; Keh, H.J. Electrophoresis of a Charged Soft Particle in a Charged Cavity with Arbitrary Double-Layer Thickness. *J. Phys. Chem. B.* **2013**, 117:9757-9767.
- (27) Happel, J. Viscous Flow in Multiparticle Systems: Slow Motion of Fluid Relative to Beds of Spherical Particles. *AIChE J.* **1958**,4:197-201.
- (28) Kuwabara, S. The Forces Experienced by Randomly Distributed Parallel Circular Cylinders or Spheres in a Viscous Flow at Small Reynolds Numbers. *J. Phys. Soc. Jpn.* **1959**,14:527-532.

# Appendix

## The constants $C_{ni}$ in Eqs. (29) and (30)



The dimensionless constants  $C_{ni}$  in Eqs. (29) and (30) for the fluid flow field are given as follows:

$$C_{1i} = \frac{1}{A_1} \{ [U_i - J_{2i}(b)]B_2 - J_{0i}(b)B_1 - J_{3i}(b)B_3 - J_{5i}(b)B_4 - J_{0i}(r_0)B_5 - J_{3i}(r_0)B_6 - J_{\alpha i}(r_0)B_7 - J_{\beta i}(r_0)B_8 \}, \quad (A1)$$

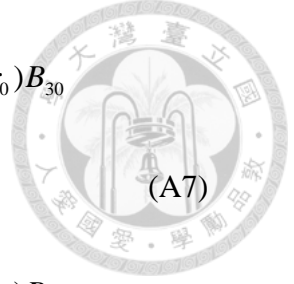
$$C_{2i} = \frac{1}{A_1} \{ [U_i - J_{2i}(b)]A_0 - J_{0i}(b)A_2 - J_{3i}(b)A_3 - J_{5i}(b)A_4 - J_{0i}(r_0)A_5 - J_{3i}(r_0)A_6 - J_{\alpha i}(r_0)A_7 - J_{\beta i}(r_0)A_8 \}, \quad (A2)$$

$$C_{3i} = \frac{1}{A_1} \{ [U_i - J_{2i}(b)]A_2 - J_{0i}(b)B_9 - J_{3i}(b)B_1 - J_{5i}(b)B_{10} - J_{0i}(r_0)B_{11} - J_{3i}(r_0)B_{12} - J_{\alpha i}(r_0)B_{13} - J_{\beta i}(r_0)B_{14} \}, \quad (A3)$$

$$C_{4i} = \frac{1}{A_1} \{ [U_i - J_{2i}(b)]A_4 - J_{0i}(b)B_{15} - J_{3i}(b)B_4 - J_{5i}(b)B_{16} - J_{0i}(r_0)B_{17} + J_{3i}(r_0)B_{18} - J_{\alpha i}(r_0)B_{19} - J_{\beta i}(r_0)B_{20} \}, \quad (A4)$$

$$C_{5i} = \frac{1}{A_1} \{ -[U_i - J_{2i}(b)]A_6 + J_{0i}(b)B_{12} + J_{3i}(b)B_6 - J_{5i}(b)B_{18} - J_{0i}(r_0)B_{21} - J_{3i}(r_0)B_{22} - J_{\alpha i}(r_0)B_{23} - J_{\beta i}(r_0)B_{24} \}, \quad (A5)$$

$$C_{6i} = \frac{1}{A_1} \{ -[U_i - J_{2i}(b)]A_5 + J_{0i}(b)B_{11} + J_{3i}(b)B_5 + J_{5i}(b)B_{17} - J_{0i}(r_0)B_{25} - J_{3i}(r_0)B_{26} - J_{\alpha i}(r_0)B_{27} - J_{\beta i}(r_0)B_{28} \}, \quad (A6)$$



$$C_{7i} = \frac{1}{A_1} \{ -[U_i - J_{2i}(b)]A_7 + J_{0i}(b)B_{13} + J_{3i}(b)B_7 - J_{5i}(b)B_{29} - J_{0i}(r_0)B_{30} - J_{3i}(r_0)B_{31} - J_{ai}(r_0)B_{32} - J_{\beta i}(r_0)B_{33} \}, \quad (A7)$$

$$C_{8i} = \frac{1}{A_1} \{ -[U_i - J_{2i}(b)]A_8 + J_{0i}(b)B_{14} + J_{3i}(b)B_8 - J_{5i}(b)B_{34} - J_{0i}(r_0)B_{35} - J_{3i}(r_0)B_{36} - J_{ai}(r_0)B_{37} - J_{\beta i}(r_0)B_{38} \}, \quad (A8)$$

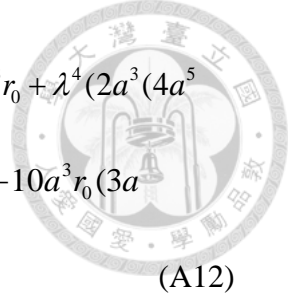
where

$$A_0 = \frac{1}{a^4} \{ -120a^6 r_0 \lambda^3 + \lambda [270a^3 r_0 (a - r_0) + a\lambda^4 (2a^5 + 3b^5)(2a^3 + r_0^3) + 3\lambda^2 (20a^7 + r_0(2a^6 + 3ab^5 - 3(4a^5 + b^5)r_0 + 30a^4 r_0^2))] \cosh(\lambda(a - r_0)) - 3[90a^3 r_0 + \lambda^4 (2a^3 (4a^5 + b^5) + r_0^2 (-2a^6 - 3ab^5 + r_0(4a^5 + b^5))) + \lambda^2 (20a^6 + 3r_0(4a^5 + b^5 + 10a^3 r_0(r_0 - 3a)))] \sinh(\lambda a - \lambda r_0) \} \quad (A9)$$

$$A_1 = \frac{1}{a^3 b} \{ -12r_0 \lambda (30a^3 b - 10a^6 \lambda^2 + 9a^5 b \lambda^2 + b^6 \lambda^2) - \lambda [\lambda^4 (a - b)^3 (a + b)(2a^2 + ab + 2b^2)(2a^3 + r_0^3) - 90a^3 (2ab + r_0(-3a + 2b + 3r_0)) + 3\lambda^2 (20a^7 - 28a^6 b - 2ab^6 + r_0(2a^6 - 3a^5 b + 3ab^5 - 2b^6 - 3(4a^5 - 5a^4 b + b^5)r_0 + 10a^3 (3a - 2b)r_0^2))] \cosh(\lambda a - \lambda r_0) + 3[30a^3 (3r_0 - 2b) + \lambda^4 (2a^3 (4a^5 - 5a^4 b + b^5) + r_0^2 (-2a^6 + 3a^5 b - 3ab^5 + 2b^6 + r_0(4a^5 - 5a^4 b + b^5))) + \lambda^2 (20a^6 - 48a^5 b - 2b^6 + 3r_0(4a^5 - 5a^4 b + b^5 + 10a^3 r_0(-3a + 2b + r_0)))] \sinh(\lambda a - \lambda r_0) \} \quad (A10)$$

$$A_2 = \frac{b^5 \lambda^2}{a^4} \{ 6ar_0 \lambda - \lambda [3(4a - 3r_0)(a + r_0) + a\lambda^2 (2a^3 + r_0^3)] \cosh(\lambda a - \lambda r_0) + 3[4a + 3r_0 + \lambda^2 (2a^3 - ar_0^2 + r_0^3)] \sinh(\lambda a - \lambda r_0) \} \quad (A11)$$

$$A_3 = \frac{1}{a^3 b} \{ 120a^6 r_0 \lambda^3 - \lambda [270a^3 r_0 (a - r_0) + a\lambda^4 (2a^5 + 3b^5)(2a^3 + r_0^3) + 3\lambda^2 (20a^7$$



$$\begin{aligned}
 &+r_0(2a^6+3ab^5-3(4a^5+b^5)r_0+30a^4r_0^2))\cosh(\lambda a-\lambda r_0)+3[90a^3r_0+\lambda^4(2a^3(4a^5 \\
 &+b^5)-r_0^2(2a^6+3ab^5-r_0(4a^5+b^5)))+\lambda^2(20a^6+3r_0(4a^5+b^5-10a^3r_0(3a \\
 &-r_0)))]\sinh(\lambda a-\lambda r_0)\} \tag{A12}
 \end{aligned}$$

$$\begin{aligned}
 A_4 = \lambda^2 a \{-6ar_0\lambda + \lambda[3(4a-3r_0)(a+r_0) + a\lambda^2(2a^3+r_0^3)]\cosh(\lambda a-\lambda r_0) - 3[4a+3r_0 + \lambda^2(2a^3 \\
 -ar_0^2+r_0^3)]\sinh(\lambda a-\lambda r_0)\} \tag{A13}
 \end{aligned}$$

$$\begin{aligned}
 A_5 = \frac{6r_0}{a^6\lambda^2} \{2a^3\lambda^5(a^5-b^5) - \lambda[90a^3(a-r_0) + ar_0^2\lambda^4(4a^5+b^5) + 3\lambda^2(a-r_0)(4a^5+b^5 \\
 -10a^4r_0)]\cosh(\lambda a-\lambda r_0) + [90a^3+r_0\lambda^4(-3a(4a^5+b^5)+r_0(14a^5+b^5)) + 3\lambda^2(14a^5 \\
 +b^5+10a^3r_0(r_0-3a))]\sinh(\lambda a-\lambda r_0)\} \tag{A14}
 \end{aligned}$$

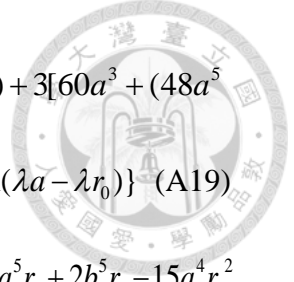
$$\begin{aligned}
 A_6 = \frac{6}{a^3r_0} \{[(a^5-b^5)\lambda^3 - 30a^3\lambda] + [30a^4\lambda + (4a^5+b^5)a\lambda^3]\cosh(\lambda a-\lambda r_0) - [30a^3 + (14a^5 \\
 +b^5)\lambda^2]\sinh(\lambda a-\lambda r_0)\} \tag{A15}
 \end{aligned}$$

$$\begin{aligned}
 A_7 = \frac{1}{a^6\lambda^2} \{[-18r_0(30a^3 + \lambda^2(14a^5 + b^5))]\cosh(\lambda a) + [12a^3(b^5 - a^5)\lambda^4 + 6r_0(30a^3 - (a^5 \\
 -b^5)\lambda^2)(3 + \lambda^2r_0^2)]\cosh(\lambda r_0) + 18ar_0\lambda[(30a^3 + (4a^5 + b^5)\lambda^2)]\sinh(\lambda a) + 18r_0^2\lambda[-30a^3 \\
 +(a^5 - b^5)\lambda^2]\sinh(\lambda r_0)\} \tag{A16}
 \end{aligned}$$

$$\begin{aligned}
 A_8 = \frac{6}{a^6\lambda^2} \{[3r_0^2\lambda(30a^3 - \lambda^2(a^5 - b^5))]\cosh(\lambda r_0) - 3ar_0\lambda[(30a^3 + (4a^5 + b^5)\lambda^2)]\cosh(\lambda a) \\
 + [2a^3(a^5 - b^5)\lambda^4 + (r_0\lambda^2(a^5 - b^5) - 30a^3)(3 + \lambda^2r_0^2)]\sinh(\lambda r_0) + 3r_0[30a^3 + (14a^5 \\
 +b^5)\lambda^2]\sinh(\lambda a)\} \tag{A17}
 \end{aligned}$$

$$\begin{aligned}
 B_1 = \frac{b^4\lambda^2}{a^3} \{-6ar_0\lambda + \lambda[3(4a-3r_0)(a+r_0) + a(2a^3+r_0^3)\lambda^2]\cosh(\lambda a-\lambda r_0) - [3(4a+3r_0 \\
 +(2a^3-ar_0^2+r_0^3)\lambda^2)]\sinh(\lambda a-\lambda r_0)\} \tag{A18}
 \end{aligned}$$

$$\begin{aligned}
 B_2 = \frac{1}{a^3} \{12r_0\lambda[30a^3 + (9a^5 + b^5)\lambda^2] - \lambda[180a^3(a+r_0) + 3(28a^6 + 2ab^5 + 3a^5r_0 + 2b^5r_0 \\
 \dots)]\}
 \end{aligned}$$



$$\begin{aligned}
 & -15a^4r_0^2 + 20a^3r_0^3)\lambda^2 + (3a^5 + 2b^5)(2a^3 + r_0^3)\lambda^4] \cosh(\lambda a - \lambda r_0) + 3[60a^3 + (48a^5 \\
 & + 2b^5 + 15a^4r_0 - 60a^3r_0^2)\lambda^2 + (10a^7 - (3a^5 + 2b^5)r_0^2 + 5a^4r_0^3)\lambda^4] \sinh(\lambda a - \lambda r_0)\} \quad (A19)
 \end{aligned}$$

$$\begin{aligned}
 B_3 = \frac{1}{a^2b} \{ & -12r_0\lambda(30a^3 + (9a^5 + b^5)\lambda^2) + \lambda[180a^3(a + r_0) + 3(28a^6 + 2ab^5 + 3a^5r_0 + 2b^5r_0 - 15a^4r_0^2 \\
 & + 20a^3r_0^3)\lambda^2 + (3a^5 + 2b^5)(2a^3 + r_0^3)\lambda^4] \cosh(\lambda a - \lambda r_0) - 3[60a^3 + \lambda^2(48a^5 + 2b^5 \\
 & + 15a^4r_0 - 60a^3r_0^2) + \lambda^4(10a^7 - (3a^5 + 2b^5)r_0^2 + 5a^4r_0^3)] \sinh(\lambda a - \lambda r_0)\} \quad (A20)
 \end{aligned}$$

$$\begin{aligned}
 B_4 = \frac{a^2\lambda^2}{b} \{ & 6ar_0\lambda - \lambda[3(4a - 3r_0)(a + r_0) + a\lambda^2(2a^3 + r_0^3)] \cosh(\lambda a - \lambda r_0) + 3[4a + 3r_0 + \lambda^2(2a^3 \\
 & - ar_0^2 + r_0^3)] \sinh(\lambda a - \lambda r_0)\} \quad (A21)
 \end{aligned}$$

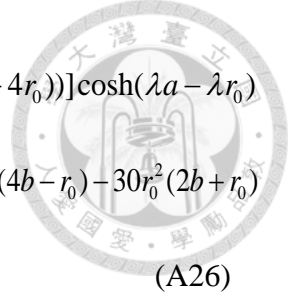
$$\begin{aligned}
 B_5 = \frac{6r_0}{a^5b\lambda^2} \{ & 2a^3\lambda^5(b^5 - a^5) + \lambda[90a^3(a - r_0) + 3\lambda^2(a - r_0)(4a^5 + b^5 - 10a^4r_0) + ar_0^2\lambda^4(4a^5 \\
 & + b^5)] \cosh(\lambda a - \lambda r_0) - [90a^3 + 3\lambda^2(b^5 + 2a^3(7a^2 - 15ar_0 + 5r_0^2)) + r_0\lambda^4(3a(b^5 - 4a^5) \\
 & + r_0(14a^5 + b^5))] \sinh(\lambda a - \lambda r_0)\} \quad (A22)
 \end{aligned}$$

$$\begin{aligned}
 B_6 = \frac{6}{a^2b} \{ & r_0\lambda(30a^3 - a^5\lambda^2 + b^5\lambda^2) - a\lambda[30a^3 + (4a^5 + b^5)\lambda^2] \cosh(\lambda a - \lambda r_0) + [30a^3 + \lambda^2(14a^5 \\
 & + b^5)] \sinh(\lambda a - \lambda r_0)\} \quad (A23)
 \end{aligned}$$

$$\begin{aligned}
 B_7 = \frac{6}{a^5b\lambda^2} \{ & 3r_0[30a^3 + \lambda^2(14a^5 + b^5)] \cosh(\lambda a) - [90a^3r_0 + 3r_0\lambda^2(10a^3r_0^2 - a^5 + b^5) - (a^5 - b^5)(2a^3 \\
 & + r_0^3)\lambda^4] \cosh(\lambda r_0) + [-3ar_0\lambda(30a^3 + (4a^5 + b^5)\lambda^2)] \sinh(\lambda a) + 3r_0^2\lambda[30a^3 - a^5\lambda^2 \\
 & + b^5\lambda^2] \sinh(\lambda r_0)\} \quad (A24)
 \end{aligned}$$

$$\begin{aligned}
 B_8 = \frac{1}{a^5b\lambda^2} \{ & [18ar_0\lambda(30a^3 + (4a^5 + b^5)\lambda^2)] \cosh(\lambda a) + 18r_0^2\lambda[(a^5 - b^5)\lambda^2 \\
 & - 30a^3] \cosh(\lambda r_0) - 18r_0[30a^3 + (14a^5 + b^5)\lambda^2] \sinh(\lambda a) - 6[-90a^3r_0 - 3r_0(10a^3r_0^2 - a^5 + b^5)\lambda^2 \\
 & + \lambda^4(a^5 - b^5)(2a^3 + r_0^3)] \sinh(\lambda r_0)\} \quad (A25)
 \end{aligned}$$

$$B_9 = \frac{-b^4}{5a^5} \{ 12\lambda(30b + a^2r_0\lambda^2(-10a + 9b)) + \lambda[-90(2ab - 3ar_0 + 2br_0 + 3r_0^2) + a^2\lambda^4(2a - 3b)(2a^3$$



$$\begin{aligned}
 &+r_0^3) + 3\lambda^2(20a^4 - 20br_0^3 + 2a^3(r_0 - 14b) + 15ar_0^2(b + 2r_0) - 3a^2r_0(b + 4r_0))\cosh(\lambda a - \lambda r_0) \\
 &+ 3[60b - 90r_0 + a\lambda^4(2a^3(5b - 4a) + ar_0^2(2a - 3b) + r_0^3(5b - 4a)) + \lambda^2(12a^2(4b - r_0) - 30r_0^2(2b + r_0) \\
 &+ 15ar_0(b + 6r_0) - 20a^3)]\sinh(\lambda a - \lambda r_0)\} \tag{A26}
 \end{aligned}$$

$$\begin{aligned}
 B_{10} = &\frac{-1}{5b}\{12\lambda(-30b + a^2r_0(10a - 9b)\lambda^2) + \lambda[90(2ab - 3ar_0 + 2br_0 + 3r_0^2) - a^2\lambda^4(2a \\
 &- 3b)(2a^3 + r_0^3) + 3\lambda^2(a^3(28b - 2r_0) - 20a^4 + 20br_0^3 - 15ar_0^2(b + 2r_0) + 3a^2r_0(b + 4r_0))]\cosh(\lambda a - \lambda r_0) \\
 &+ 3[90r_0 - 60b + a\lambda^4(2a^3(4a - 5b) + ar_0^2(3b - 2a) + r_0^3(4a - 5b)) + \lambda^2(20a^3 + 12a^2(r_0 - 4b) + 30r_0^2(2b + r_0) \\
 &- 15ar_0(b + 6r_0))]\sinh(\lambda a - \lambda r_0)\} \tag{A27}
 \end{aligned}$$

$$\begin{aligned}
 B_{11} = &\frac{-6b^4r_0}{a^6}\{2a^3\lambda^3(a - b) - 6ab\lambda + \lambda[a(b - 2a)\lambda^2r_0^2 + 3(br_0 - 2a^2 + a(b \\
 &+ 2r_0))]\cosh(\lambda a - \lambda r_0) + [6a + 3b + r_0\lambda^2(3ab + 2ar_0 + br_0 - 6a^2)]\sinh(\lambda a - \lambda r_0)\} \tag{A28}
 \end{aligned}$$

$$B_{12} = \frac{6b^4\lambda^2}{a^3}\{r_0\lambda(b - a) + a\lambda(b - 2a)\cosh(\lambda a - \lambda r_0) + (2a + b)\sinh(\lambda a - \lambda r_0)\} \tag{A29}$$

$$\begin{aligned}
 B_{13} = &\frac{6b^4}{a^6}\{[3ar_0 - 6ab - 3br_0 + \lambda^2(a - b)(2a^3 + r_0^3)]\cosh(\lambda r_0) + [3r_0(2a + b)]\cosh(\lambda a) \\
 &+ [3r_0^2\lambda(b - a)]\sinh(\lambda r_0) + [3ar_0\lambda(b - 2a)]\sinh(\lambda a)\} \tag{A30}
 \end{aligned}$$

$$\begin{aligned}
 B_{14} = &\frac{-6b^4}{a^6}\{[3r_0^2\lambda(b - a)]\cosh(\lambda r_0) + [3ar_0\lambda(b - 2a)]\cosh(\lambda a) + [3a(-2b + r_0) - 3br_0 \\
 &+ (a - b)\lambda^2(2a^3 + r_0^3)]\sinh(\lambda r_0) + [3r_0(2a + b)]\sinh(\lambda a)\} \tag{A31}
 \end{aligned}$$

$$\begin{aligned}
 B_{15} = &\frac{-\lambda^2}{5a^3b}\{12b^6r_0\lambda + \lambda[9ar_0 - 6ab - 6br_0 - 9r_0^2 + (3a - 2b)\lambda^2(2a^3 + r_0^3)]\cosh(\lambda a - \lambda r_0) \\
 &- 3b^5[3r_0 - 2b + \lambda^2(2a^3 - 3ar_0^2 + 2br_0^2 + r_0^3)]\sinh(\lambda a - \lambda r_0)\} \tag{A32}
 \end{aligned}$$

$$\begin{aligned}
 B_{16} = &\frac{-a^2\lambda^2}{5b}\{-12br_0\lambda + \lambda[6ab - 9ar_0 + 6br_0 + 9r_0^2 - (3a - 2b)\lambda^2(2a^3 + r_0^3)]\cosh(\lambda a - \lambda r_0) \\
 &+ 3[3r_0 - 2b + \lambda^2(2a^3 - 3ar_0^2 + 2br_0^2 + r_0^3)]\sinh(\lambda a - \lambda r_0)\} \tag{A33}
 \end{aligned}$$

$$B_{17} = \frac{6r_0}{ab}\{2a^3(a - b)\lambda^3 - 6ab\lambda + \lambda[ar_0^2\lambda^2(b - 2a) + 3(br_0 - 2a^2 + a(b$$



$$+2r_0))\cosh(\lambda a - \lambda r_0) + [6a + 3b + r_0\lambda^2(3ab - 6a^2 + 2ar_0 + br_0)]\sinh(\lambda a - \lambda r_0)\} \quad (\text{A34})$$

$$B_{18} = \frac{6a^2\lambda^2}{b} \{r_0\lambda(a - b) + [a\lambda(2a - b)]\cosh(\lambda a - \lambda r_0) - (2a + b)\sinh(\lambda a - \lambda r_0)\} \quad (\text{A35})$$

$$B_{19} = \frac{-6}{ab} \{ [3ar_0 - 6ab - 3br_0 + \lambda^2(a - b)(2a^3 + r_0^3)]\cosh(\lambda r_0) + [3r_0(2a + b)]\cosh(\lambda a) \\ + 3\lambda r_0^2(b - a)\sinh(\lambda r_0) + 3ar_0\lambda(b - 2a)\sinh(\lambda a) \} \quad (\text{A36})$$

$$B_{20} = \frac{6}{ab} \{ 3r_0^2\lambda(b - a)\cosh(\lambda r_0) + [3ar_0\lambda(b - 2a)]\cosh(\lambda a) + [3a(r_0 - 2b) - 3br_0 \\ + \lambda^2(a - b)(2a^3 + r_0^3)]\sinh(\lambda r_0) + [3r_0(2a + b)]\sinh(\lambda a) \} \quad (\text{A37})$$

$$B_{21} = \frac{2r_0}{a^5b\lambda^2} \{ 180a^3b\lambda + 6\lambda^3(9a^5b - 10a^6 + b^6) + \lambda[90a^3(3a - 2b - 3r_0) + (2a^6 - 3a^5b + 3ab^5 \\ - 2b^6)\lambda^4r_0^2 + 3\lambda^2(2a^6 + 3ab^5 - 20a^3br_0^2 + 15a^4r_0(b + 2r_0) - b^5(2b + 3r_0) - 3a^5(b \\ + 4r_0))] \cosh(\lambda a - \lambda r_0) - 3[90a^3 + r_0\lambda^4(-2a^6 - 3ab^5 - 5a^4br_0 + b^5(2b + r_0) + a^5(3b + 4r_0)) + 3\lambda^2(4a^5 \\ + b^5 + 10a^3r_0(2b + r_0) - 5a^4(b + 6r_0))] \sinh(\lambda a - \lambda r_0) \} \quad (\text{A38})$$

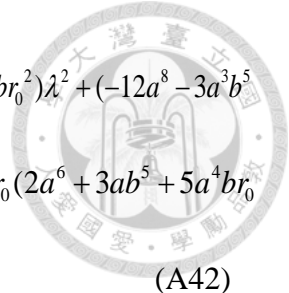
$$B_{22} = \frac{-2}{a^2b} \{ \lambda[30a^3(3a - 2b) + (2a^6 - 3a^5b + 3ab^5 - 2b^6)\lambda^2] \cosh(\lambda a - \lambda r_0) \\ - 3[30a^3 + 4a^5\lambda^2 - 5a^4b\lambda^2 + b^5\lambda^2] \sinh(\lambda a - \lambda r_0) \} \quad (\text{A39})$$

$$B_{23} = \frac{-6}{a^5b\lambda^2} \{ 2[30a^3b - 10a^6\lambda^2 + 9a^5b\lambda^2 + b^6\lambda^2] \cosh(\lambda r_0) - 3r_0[30a^3 + 4a^5\lambda^2 - 5a^4b\lambda^2 \\ + b^5\lambda^2] \cosh(\lambda a) + r_0\lambda[30a^3(3a - 2b) + (2a^6 - 3a^5b + 3ab^5 - 2b^6)\lambda^2] \sinh(\lambda a) \} \quad (\text{A40})$$

$$B_{24} = \frac{6}{a^5b\lambda^2} \{ (r_0\lambda(30a^3(3a - 2b) + (2a^6 - 3a^5b + 3ab^5 - 2b^6)\lambda^2) \cosh(\lambda a) \\ - 3r_0(30a^3 + 4a^5\lambda^2 - 5a^4b\lambda^2 + b^5\lambda^2) \sinh(\lambda a) + 2(30a^3b - 10a^6\lambda^2 + 9a^5b\lambda^2 \\ + b^6\lambda^2) \sinh(\lambda r_0) \} \quad (\text{A41})$$

$$B_{25} = \frac{-4r_0}{a^8b\lambda^4} \{ \lambda(270a^3b(a - r_0) - 9(a - r_0)(10a^6 - 14a^5b - b^6 + 10a^4br_0))\lambda^2 + 3a(-2a^8 - 3a^3b^5 \\ + 14a^5br_0^2 + b^6r_0^2 - 5a^6r_0(3b + 2r_0) + a^2b^5(2b + 3r_0) + 3a^7(b + 4r_0))\lambda^4 + a^3(-2a^6 + 3a^5b - 3ab^5$$





$$\begin{aligned}
& +2b^6r_0^2\lambda^6)\cosh(\lambda a-\lambda r_0)-3(90a^3b+3(-10a^6+24a^5b+b^6-30a^4br_0+10a^3br_0^2)\lambda^2+(-12a^8-3a^3b^5 \\
& -3ab^6r_0+24a^5br_0^2+b^6r_0^2+15a^7(b+2r_0)-2a^6r_0(21b+5r_0))\lambda^4+a^3r_0(2a^6+3ab^5+5a^4br_0 \\
& -b^5(2b+r_0)-a^5(3b+4r_0))\lambda^6)\sinh(\lambda a-\lambda r_0)] \tag{A42}
\end{aligned}$$

$$\begin{aligned}
B_{26} &= \frac{-4}{a^5b\lambda^2}[90a^3br_0\lambda+3(-10a^6+9a^5b+b^6)r_0\lambda^3+a\lambda(-90a^3b+3(10a^6-14a^5b-b^6)\lambda^2 \\
& +a^2(2a^6-3a^5b+3ab^5-2b^6)\lambda^4)\cosh(\lambda a-\lambda r_0)+3(-10a^6\lambda^2+24a^5b\lambda^2+b^6\lambda^2-4a^8\lambda^4 \\
& +5a^7b\lambda^4+a^3b(30-b^4\lambda^4))\sinh(\lambda a-\lambda r_0)] \tag{A43}
\end{aligned}$$

$$\begin{aligned}
B_{27} &= \frac{12r_0}{a^8b\lambda^4}\{3[10a^6\lambda^2-24a^5b\lambda^2-b^6\lambda^2+4a^8\lambda^4-5a^7b\lambda^4+a^3b(b^4\lambda^4-30)]\cosh(\lambda a) \\
& +\lambda a[90a^3b-3\lambda^2(10a^6-14a^5b-b^6)-\lambda^4a^2(2a^6-3a^5b+3ab^5-2b^6)]\sinh(\lambda a) \\
& +[30a^3b-\lambda^2(10a^6-9a^5b-b^6)][(3+\lambda^2r_0^2)\cosh(\lambda r_0)-3\lambda r_0\sinh(\lambda r_0)]\} \tag{A44}
\end{aligned}$$

$$\begin{aligned}
B_{28} &= \frac{-12r_0}{a^8b\lambda^4}\{[90a^4b\lambda-3\lambda^3a(10a^6-14a^5b-b^6)-\lambda^5a^3(2a^6-3a^5b+3ab^5-2b^6)]\cosh(\lambda a) \\
& +3[10a^6\lambda^2-24a^5b\lambda^2-b^6\lambda^2+4a^8\lambda^4-5a^7b\lambda^4-a^3b(30-b^4\lambda^4)]\sinh(\lambda a)+[30a^3b \\
& -(10a^6-9a^5b-b^6)\lambda^2][ -3\lambda r_0\cosh(\lambda r_0)+(3+r_0^2\lambda^2)\sinh(\lambda r_0)]\} \tag{A45}
\end{aligned}$$

$$\begin{aligned}
B_{29} &= \frac{6}{ab}\{3(2a+b)r_0\cosh(\lambda a)-[6ab-3ar_0+3br_0-(a-b)(2a^3+r_0^3)\lambda^2]\cosh(\lambda r_0) \\
& -3r_0\lambda[a(2a-b)\sinh(\lambda a)+(a-b)r_0\sinh(\lambda r_0)]\} \tag{A46}
\end{aligned}$$

$$\begin{aligned}
B_{30} &= \frac{12r_0}{a^8b\lambda^4}\{3[10a^6\lambda^2-24a^5b\lambda^2-b^6\lambda^2+4a^8\lambda^4-5a^7b\lambda^4+a^3b(-30+b^4\lambda^4)]\cosh(\lambda a) \\
& +\lambda a[90a^3b-3(10a^6-14a^5b-b^6)\lambda^2-a^2(2a^6-3a^5b+3ab^5-2b^6)\lambda^4]\sinh(\lambda a) \\
& +[30a^3b-(10a^6-9a^5b-b^6)\lambda^2][(3+r_0^2\lambda^2)\cosh(\lambda r_0)-3r_0\lambda\sinh(\lambda r_0)]\} \tag{A47}
\end{aligned}$$

$$\begin{aligned}
B_{31} &= \frac{-6}{a^5b\lambda^2}\{-3r_0(30a^3+4a^5\lambda^2-5a^4b\lambda^2+b^5\lambda^2)\cosh(\lambda a)+2(30a^3b-10a^6\lambda^2+9a^5b\lambda^2 \\
& +b^6\lambda^2)\cosh(\lambda r_0)+r_0\lambda[30a^3(3a-2b)+(2a^6-3a^5b+3ab^5-2b^6)\lambda^2]\sinh(\lambda a)\} \tag{A48}
\end{aligned}$$



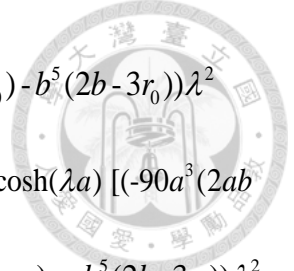
$$\begin{aligned}
 B_{32} = & \frac{-6}{a^8 b \lambda^5} \{ \cosh(\lambda r_0) [3(30a^3(-2b+3r_0) + (20a^6 - 15a^4 b r_0 + 30a^3 r_0^3 - 12a^5(4b-r_0) \\
 & - b^5(2b-3r_0))\lambda^2 + (a-b)^2(4a^3 + 3a^2b + 2ab^2 + b^3)(2a^3 + r_0^3)\lambda^4) \cosh(\lambda a) \\
 & + \lambda(90a^3(2ab - 3ar_0 + 2br_0) + 3(-20a^7 + ab^5(2b-3r_0) + 2a^6(14b-r_0) + 3a^5br_0 + 2b^6r_0 \\
 & - 30a^4r_0^3 + 20a^3br_0^3)\lambda^2 - (a-b)^3(a+b)(2a^2 + ab + 2b^2)(2a^3 + r_0^3)\lambda^4) \sinh(\lambda a)] \\
 & + 3r_0^2 \lambda [-3(30a^3 + 4a^5 \lambda^2 - 5a^4 b \lambda^2 + b^5 \lambda^2) \cosh(\lambda a) + \lambda(30a^3(3a-2b) + (2a^6 - 3a^5 b \\
 & + 3ab^5 - 2b^6)\lambda^2) \sinh(\lambda a)] \sinh(\lambda r_0) \} \tag{A49}
 \end{aligned}$$

$$\begin{aligned}
 B_{33} = & \frac{-6}{a^8 b \lambda^5} \{ 6r_0 \lambda [-30a^3 b + (10a^6 - 9a^5 b - b^6)\lambda^2] + 3r_0^2 \lambda \cosh(\lambda r_0) [3(30a^3 + 4a^5 \lambda^2 - 5a^4 b \lambda^2 \\
 & + b^5 \lambda^2) \cosh(\lambda a) + \lambda(-90a^4 + 60a^3 b - 2a^6 \lambda^2 + 3a^5 b \lambda^2 - 3ab^5 \lambda^2 + 2b^6 \lambda^2) \sinh(\lambda a)] \\
 & + [-3(30a^3(-2b+3r_0) + (20a^6 - 15a^4 b r_0 + 30a^3 r_0^3 + 12a^5(-4b+r_0) + b^5(-2b+3r_0))\lambda^2 \\
 & + (a-b)^2(4a^3 + 3a^2b + 2ab^2 + b^3)(2a^3 + r_0^3)\lambda^4) \cosh(\lambda a) + \lambda(-90a^3(2ab - 3ar_0 + 2br_0) \\
 & + 3(20a^7 - 3a^5 b r_0 - 2b^6 r_0 + 30a^4 r_0^3 - 20a^3 b r_0^3 + 2a^6(-14b+r_0) + ab^5(-2b+3r_0))\lambda^2 \\
 & + (a-b)^3(a+b)(2a^2 + ab + 2b^2)(2a^3 + r_0^3)\lambda^4) \sinh(\lambda a)] \sinh(\lambda r_0) \} \tag{A50}
 \end{aligned}$$

$$\begin{aligned}
 B_{34} = & \frac{-6}{ab} \{ 3r_0 [a(-2a+b)\lambda \cosh(\lambda a) - (a-b)r_0 \lambda \cosh(\lambda r_0) + (2a+b) \sinh(\lambda a)] \\
 & + [-3br_0 - 3a(2b-r_0) + (a-b)(2a^3 + r_0^3)\lambda^2] \sinh(\lambda r_0) \} \tag{A51}
 \end{aligned}$$

$$\begin{aligned}
 B_{35} = & \frac{-12r_0}{a^8 b \lambda^4} \{ [90a^4 b \lambda - 3a(10a^6 - 14a^5 b - b^6)\lambda^3 - a^3(2a^6 - 3a^5 b + 3ab^5 - 2b^6)\lambda^5] \cosh(\lambda a) \\
 & + 3 [10a^6 \lambda^2 - 24a^5 b \lambda^2 - b^6 \lambda^2 + 4a^8 \lambda^4 - 5a^7 b \lambda^4 + a^3 b(-30 + b^4 \lambda^4)] \sinh(\lambda a) + [30a^3 b \\
 & - (10a^6 - 9a^5 b - b^6)\lambda^2] [-3r_0 \lambda \cosh(\lambda r_0) + (3+r_0^2 \lambda^2) \sinh(\lambda r_0)] \} \tag{A52}
 \end{aligned}$$

$$\begin{aligned}
 B_{36} = & \frac{6}{a^5 b \lambda^2} \{ r_0 \lambda [30a^3(3a-2b) + (2a^6 - 3a^5 b + 3ab^5 - 2b^6)\lambda^2] \cosh(\lambda a) - 3r_0(30a^3 + 4a^5 \lambda^2 \\
 & - 5a^4 b \lambda^2 + b^5 \lambda^2) \sinh(\lambda a) + 2(30a^3 b - 10a^6 \lambda^2 + 9a^5 b \lambda^2 + b^6 \lambda^2) \sinh(\lambda r_0) \} \tag{A53}
 \end{aligned}$$



$$\begin{aligned}
 B_{37} = & \frac{-6}{a^8 b \lambda^5} \{ -3[30a^3(-2b+3r_0) + (20a^6 - 15a^4br_0 + 30a^3r_0^3 - 12a^5(4b-r_0) - b^5(2b-3r_0))\lambda^2 \\
 & + (a-b)^2(4a^3 + 3a^2b + 2ab^2 + b^3)(2a^3 + r_0^3)\lambda^4] \cosh(\lambda r_0) \sinh(\lambda a) + \lambda \cosh(\lambda a) [(-90a^3(2ab \\
 & - 3ar_0 + 2br_0) + 3(20a^7 - 3a^5br_0 - 2b^6r_0 + 30a^4r_0^3 - 20a^3br_0^3 - 2a^6(14b-r_0) - ab^5(2b-3r_0))\lambda^2 \\
 & + (a-b)^3(a+b)(2a^2 + ab + 2b^2)(2a^3 + r_0^3)\lambda^4] \cosh(\lambda r_0) + 3r_0^2\lambda(-90a^4 + 60a^3b - 2a^6\lambda^2 \\
 & + 3a^5b\lambda^2 - 3ab^5\lambda^2 + 2b^6\lambda^2) \sinh(\lambda r_0)] + 3r_0\lambda[60a^3b + 2(-10a^6 + 9a^5b + b^6)\lambda^2 + 3r_0(30a^3 \\
 & + 4a^5\lambda^2 - 5a^4b\lambda^2 + b^5\lambda^2) \sinh(\lambda a) \sinh(\lambda r_0)] \} \tag{A54}
 \end{aligned}$$

$$\begin{aligned}
 B_{38} = & \frac{-6}{a^8 b \lambda^5} \{ 3r_0^2\lambda \cosh(\lambda r_0) [\lambda(30a^3(3a-2b) + (2a^6 - 3a^5b + 3ab^5 - 2b^6)\lambda^2) \cosh(\lambda a) \\
 & - 3(30a^3 + 4a^5\lambda^2 - 5a^4b\lambda^2 + b^5\lambda^2) \sinh(\lambda a)] + [\lambda(90a^3(2ab - 3ar_0 + 2br_0) + 3(-20a^7 \\
 & + ab^5(2b-3r_0) + a^6(28b-2r_0) + 3a^5br_0 + 2b^6r_0 - 30a^4r_0^3 + 20a^3br_0^3)\lambda^2 - (a-b)^3(a \\
 & + b)(2a^2 + ab + 2b^2)(2a^3 + r_0^3)\lambda^4) \cosh(\lambda a) + 3(30a^3(-2b+3r_0) + (20a^6 - 15a^4br_0 \\
 & + 30a^3r_0^3 - 12a^5(4b-r_0) - b^5(2b-3r_0))\lambda^2 + (a-b)^2(4a^3 + 3a^2b + 2ab^2 + b^3)(2a^3 \\
 & + r_0^3)\lambda^4) \sinh(\lambda a)] \sinh(\lambda r_0) \} \tag{A55}
 \end{aligned}$$

for the Happel model;

$$\begin{aligned}
 A_0 = & \frac{1}{a} \{ \lambda[3(a-r_0)r_0 + a(2a^3 + r_0^3)\lambda^2] \cosh(\lambda a - \lambda r_0) - [3r_0 + (2a^3 - 3ar_0^2 \\
 & + r_0^3)\lambda^2] \sinh(\lambda a - \lambda r_0) \} \tag{A56}
 \end{aligned}$$

$$\begin{aligned}
 A_1 = & \frac{-2}{15 b^6 \lambda^2} \{ 30(-2a^6 + a^3b^3 + b^6)r_0\lambda^3 + \lambda[135a^3(a-r_0)r_0 + 3(10a^7 + a^6r_0 - 5a^3b^3r_0 - 6a^5r_0^2 \\
 & + 15a^2b^3r_0^2 - ab^5(5b-9r_0) - b^5r_0(5b+9r_0) + 5a^4(-4b^3 + 3r_0^3))\lambda^2 + (a-b)^3(a^3 + 3a^2b \\
 & + 6ab^2 + 5b^3)(2a^3 + r_0^3)\lambda^4] \cosh(\lambda a - \lambda r_0) - 3[45a^3r_0 + (10a^6 + 6a^5r_0 - 15a^2b^3r_0 - 45a^4r_0^2 \\
 & - b^5(5b-9r_0) - 5a^3(4b^3 - 3r_0^3))\lambda^2 + (4a^8 - a^6r_0^2 - 9ab^5r_0^2 - 5a^2b^3r_0^3 + b^5r_0^2(5b+3r_0) + a^3(6b^5 + 5b^3r_0^2)
 \end{aligned}$$



$$+2a^5(-5b^3 + r_0^3))\lambda^4] \sinh(\lambda a - \lambda r_0) \} \quad (A57)$$

$$A_2 = \frac{1}{15ab^3\lambda^2} \{30a(-4a^3 + b^3)r_0\lambda^3 + \lambda[270a(a - r_0)r_0 + 3(20a^5 + 2a^4r_0 - 5ab^3r_0 - 12a^3r_0^2 + 15b^3r_0^2 - a^2(20b^3 - 30r_0^3))\lambda^2 a(2a^3 - 5b^3)(2a^3 + r_0^3)\lambda^4] \cosh(\lambda a - \lambda r_0) - 3[90ar_0 + (20a^4 - 20ab^3 + 12a^3r_0 - 15b^3r_0 - 90a^2r_0^2 + 30ar_0^3)\lambda^2 + (8a^6 - 2a^4r_0^2 + 5ab^3r_0^2 - 5b^3r_0^3 + a^3(-10b^3 + 4r_0^3))\lambda^4] \sinh(\lambda a - \lambda r_0) \} \quad (A58)$$

$$A_3 = \frac{1}{15b^6\lambda^2} \{30a^3(4a^3 - b^3)r_0\lambda^3 - \lambda(270a^3(a - r_0)r_0 + 3(20a^4(a^3 - b^3) + a(2a^5 - 5a^2b^3 + 18b^5)r_0 - 3(4a^5 - 5a^2b^3 + 6b^5)r_0^2 + 30a^4r_0^3)\lambda^2 + a(2a^5 - 5a^2b^3 + 18b^5)(2a^3 + r_0^3)\lambda^4) \cosh(\lambda a - \lambda r_0) + 3(90a^3r_0 + (20a^3(a^3 - b^3) + 3(4a^5 - 5a^2b^3 + 6b^5)r_0 - 90a^4r_0^2 + 30a^3r_0^3)\lambda^2 + (2a^3(4a^5 - 5a^2b^3 + 6b^5) + a(-2a^5 + 5a^2b^3 - 18b^5)r_0^2 + (4a^5 - 5a^2b^3 + 6b^5)r_0^3)\lambda^4) \sinh(\lambda a - \lambda r_0) \} \quad (A59)$$

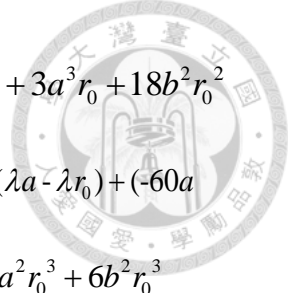
$$A_4 = \frac{a^2}{5b^3} \{ \lambda[3(a - r_0)r_0 + a(2a^3 + r_0^3)\lambda^2] \cosh(\lambda a - \lambda r_0) - [3r_0 + (2a^3 - 3ar_0^2 + r_0^3)\lambda^2] \sinh(\lambda a - \lambda r_0) \} \quad (A60)$$

$$A_5 = \frac{2r_0}{a^3b^3\lambda^2} \{ 2a^3(a^3 - b^3)\lambda^3 + (2a^3 + b^3)[- \lambda(-3r_0 + a(3 + r_0^2\lambda^2)) \cosh(\lambda a - \lambda r_0) + (3 + r_0(-3a + r_0)\lambda^2) \sinh(\lambda a - \lambda r_0)] \} \quad (A61)$$

$$A_6 = \frac{2}{b^3} \{ (a^3 - b^3)r_0\lambda + (2a^3 + b^3)[\lambda a \cosh(\lambda a - \lambda r_0) - \sinh(\lambda a - \lambda r_0)] \} \quad (A62)$$

$$A_7 = \frac{2}{a^3b^3\lambda^2} \{ (-a^3 + b^3)(3r_0 + (2a^3 + r_0^3)\lambda^2) \cosh(\lambda r_0) + 3(2a^3 + b^3)r_0(-\cosh(\lambda a) + \lambda a \sinh(\lambda a)) + 3(a^3 - b^3)r_0^2\lambda \sinh(\lambda r_0) \} \quad (A63)$$

$$A_8 = \frac{2}{a^3b^3\lambda^2} \{ -3a(2a^3 + b^3)r_0\lambda \cosh(\lambda a) + 3(2a^3 + b^3)r_0 \sinh(\lambda a) + (a^3 - b^3)[-3r_0^2\lambda \cosh(\lambda r_0) + (3r_0 + (2a^3 + r_0^3)\lambda^2) \sinh(\lambda r_0)] \} \quad (A64)$$



$$\begin{aligned}
 B_1 = & \frac{-1}{5 b^3 \lambda^2} \{ 12 a r_0 \lambda (-10 + (-3 a^2 + b^2) \lambda^2) + \lambda (60 a (a + r_0) + (28 a^4 + 3 a^3 r_0 + 18 b^2 r_0^2 \\
 & - 3 a^2 (8 b^2 + 5 r_0^2) + a (-6 b^2 r_0 + 20 r_0^3)) \lambda^2 + a (a^2 - 2 b^2) (2 a^3 + r_0^3) \lambda^4 \} \cosh (\lambda a - \lambda r_0) + (-60 a \\
 & + 3 (-16 a^3 + 8 a b^2 - 5 a^2 r_0 + 6 b^2 r_0 + 20 a r_0^2) \lambda^2 + (-10 a^5 - 6 a b^2 r_0^2 - 5 a^2 r_0^3 + 6 b^2 r_0^3 \\
 & + 3 a^3 (4 b^2 + r_0^2)) \lambda^4 \} \sinh (\lambda a - \lambda r_0) \quad (A65)
 \end{aligned}$$

$$\begin{aligned}
 B_2 = & \frac{1}{3 b^3} \{ 6 (a^3 + 2 b^3) r_0 \lambda - \lambda (3 (a + r_0) (4 a^3 + 2 b^3 - 3 a^2 r_0) + (a^3 + 2 b^3) (2 a^3 + r_0^3) \lambda^2) \cosh (\lambda a - \lambda r_0) \\
 & + 3 (4 a^3 + 2 b^3 + 3 a^2 r_0 + (2 a^5 - (a^3 + 2 b^3) r_0^2 + a^2 r_0^3) \lambda^2) \sinh (\lambda a - \lambda r_0) \} \quad (A66)
 \end{aligned}$$

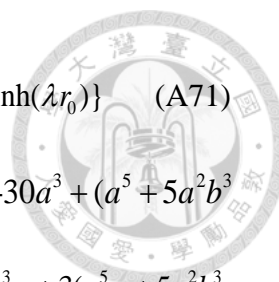
$$\begin{aligned}
 B_3 = & \frac{-a}{5 b^6 \lambda^2} \{ 12 r_0 \lambda (10 a^3 + (3 a^5 + 2 b^5) \lambda^2) - \lambda (60 a^3 (a + r_0) + (28 a^6 + 12 a b^5 + 3 a^5 r_0 \\
 & + 12 b^5 r_0 - 15 a^4 r_0^2 + 20 a^3 r_0^3) \lambda^2 + (a^5 + 4 b^5) (2 a^3 + r_0^3) \lambda^4 \} \cosh (\lambda a - \lambda r_0) + (60 a^3 + 3 (16 a^5 \\
 & + 4 b^5 + 5 a^4 r_0 - 20 a^3 r_0^2) \lambda^2 + (10 a^7 - 3 (a^5 + 4 b^5) r_0^2 + 5 a^4 r_0^3) \lambda^4) \sinh (\lambda a - \lambda r_0) \} \quad (A67)
 \end{aligned}$$

$$\begin{aligned}
 B_4 = & \frac{-a^3}{15 b^6} \{ -6 (a^3 + 2 b^3) r_0 \lambda + \lambda (3 (a + r_0) (4 a^3 + 2 b^3 - 3 a^2 r_0) + (a^3 + 2 b^3) (2 a^3 + r_0^3) \lambda^2) \cosh (\lambda a - \lambda r_0) \\
 & - 3 (4 a^3 + 2 b^3 + 3 a^2 r_0 + (2 a^5 - (a^3 + 2 b^3) r_0^2 + a^2 r_0^3) \lambda^2) \sinh (\lambda a - \lambda r_0) \} \quad (A68)
 \end{aligned}$$

$$\begin{aligned}
 B_5 = & \frac{-2 r_0}{5 a^2 b^6 \lambda^4} \{ 2 a^3 \lambda^3 (15 b^3 + (a^5 + 5 a^2 b^3 - 6 b^5) \lambda^2) - \lambda (90 a^3 (a - r_0) + 3 (4 a^6 + 5 a^3 b^3 \\
 & + 6 a b^5 - 14 a^5 r_0 + 5 a^2 b^3 r_0 - 6 b^5 r_0 + 10 a^4 r_0^2) \lambda^2 + a (4 a^5 + 5 a^2 b^3 + 6 b^5) r_0^2 \lambda^4 \} \cosh (\lambda a - \lambda r_0) \\
 & + (90 a^3 + 3 (14 a^5 - 5 a^2 b^3 + 6 b^5 - 30 a^4 r_0 + 10 a^3 r_0^2) \lambda^2 + r_0 (-3 a (4 a^5 + 5 a^2 b^3 + 6 b^5) \\
 & + (14 a^5 - 5 a^2 b^3 + 6 b^5) r_0) \lambda^4) \sinh (\lambda a - \lambda r_0) \} \quad (A69)
 \end{aligned}$$

$$\begin{aligned}
 B_6 = & \frac{-2 a}{5 b^6 \lambda^2} \{ -30 a^3 r_0 \lambda + (a^5 + 5 a^2 b^3 - 6 b^5) r_0 \lambda^3 + a \lambda (30 a^3 + (4 a^5 + 5 a^2 b^3 \\
 & + 6 b^5) \lambda^2) \cosh (\lambda a - \lambda r_0) - (30 a^3 + (14 a^5 - 5 a^2 b^3 + 6 b^5) \lambda^2) \sinh (\lambda a - \lambda r_0) \} \quad (A70)
 \end{aligned}$$

$$\begin{aligned}
 B_7 = & \frac{-1}{5 a^2 b^6 \lambda^4} \{ -6 r_0 (30 a^3 + (14 a^5 - 5 a^2 b^3 + 6 b^5) \lambda^2) \cosh (\lambda a) - 2 (-90 a^3 r_0 + 3 (a^5 r_0 \\
 & + 5 a^2 b^3 r_0 - 6 b^5 r_0 + 10 a^3 (b^3 - r_0^3)) \lambda^2 + (a^5 + 5 a^2 b^3 - 6 b^5) (2 a^3 + r_0^3) \lambda^4 \} \cosh (\lambda r_0) + 6 r_0 \lambda (a (30 a^3
 \end{aligned}$$



$$+(4a^5 + 5a^2b^3 + 6b^5)\lambda^2 \sinh(\lambda a) + r_0(-30a^3 + (a^5 + 5a^2b^3 - 6b^5)\lambda^2) \sinh(\lambda r_0) \} \quad (A71)$$

$$B_8 = \frac{1}{5a^2b^6\lambda^4} \{ 6r_0(a\lambda(30a^3 + (4a^5 + 5a^2b^3 + 6b^5)\lambda^2) \cosh(\lambda a) + \lambda r_0(-30a^3 + (a^5 + 5a^2b^3 - 6b^5)\lambda^2) \cosh(\lambda r_0) - (30a^3 + (14a^5 - 5a^2b^3 + 6b^5)\lambda^2) \sinh(\lambda a) - 2(-90a^3r_0 + 3(a^5r_0 + 5a^2b^3r_0 - 6b^5r_0 + 10a^3(b^3 - r_0^3))\lambda^2 + (a^5 + 5a^2b^3 - 6b^5)(2a^3 + r_0^3)\lambda^4) \sinh(\lambda r_0) \} \quad (A72)$$

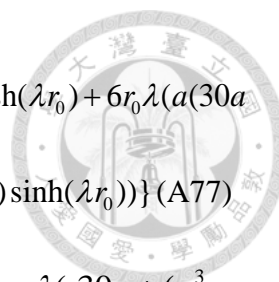
$$B_9 = \frac{1}{25a^2b\lambda^2} \{ 60r_0\lambda(-10b + a^2(4a - 3b)\lambda^2) + \lambda(60(5ab - 9ar_0 + 5br_0 + 9r_0^2) + (20a^3(-6a + 7b) + 3a^2(-4a + 5b)r_0 + 3a(24a - 25b)r_0^2 + 20(-9a + 5b)r_0^3)\lambda^2 - a^2(4a - 5b)(2a^3 + r_0^3)\lambda^4) \cosh(\lambda a - \lambda r_0) + (60(-5b + 9r_0) + 3(40a^2(a - 2b) + a(24a - 25b)r_0 + 20(-9a + 5b)r_0^2 + 60r_0^3)\lambda^2 + a(2a^3(24a - 25b) + 3a(-4a + 5b)r_0^2 + (24a - 25b)r_0^3)\lambda^4) \sinh(\lambda a - \lambda r_0) \} \quad (A73)$$

$$B_{10} = \frac{-a^2}{75b^6\lambda^2} \{ 30a(4a^3 - b^3)r_0\lambda^3 + \lambda(270ar_0(-a + r_0) - 3(20a^5 + 2a^4r_0 - 5ab^3r_0 - 12a^3r_0^2 + 15b^3r_0^2 + a^2(-20b^3 + 30r_0^3))\lambda^2 - a(2a^3 - 5b^3)(2a^3 + r_0^3)\lambda^4) \cosh(\lambda a - \lambda r_0) + 3(90ar_0 + (20a^4 - 20ab^3 + 12a^3r_0 - 15b^3r_0 - 90a^2r_0^2 + 30ar_0^3)\lambda^2 + (8a^6 - 2a^4r_0^2 + 5ab^3r_0^2 - 5b^3r_0^3 + a^3(-10b^3 + 4r_0^3))\lambda^4) \sinh(\lambda a - \lambda r_0) \} \quad (A74)$$

$$B_{11} = \frac{2r_0}{5a^3b^3\lambda^4} \{ 30ab^3\lambda^3 + 2a^3(a^3 - 6ab^2 + 5b^3)\lambda^5 - \lambda(90a(a - r_0) + 3(4a^4 - 14a^3r_0 + 5b^3r_0 + ab^2(5b + 12r_0) + 2a^2(-6b^2 + 5r_0^2))\lambda^2 + a(4a^3 - 12ab^2 + 5b^3)r_0^2\lambda^4) \cosh(\lambda a - \lambda r_0) - (-90a + 3(-14a^3 + 5b^3 + 30a^2r_0 + 2a(6b^2 - 5r_0^2))\lambda^2 + r_0(12a^4 - 36a^2b^2 - 14a^3r_0 + 5b^3r_0 + 3ab^2(5b + 4r_0))\lambda^4) \sinh(\lambda a - \lambda r_0) \} \quad (A75)$$

$$B_{12} = \frac{2}{5b^3\lambda^2} \{ -30ar_0\lambda + (a^3 - 6ab^2 + 5b^3)r_0\lambda^3 + a\lambda(30a + (4a^3 - 12ab^2 + 5b^3)\lambda^2) \cosh(\lambda a - \lambda r_0) + (-30a + (-14a^3 + 12ab^2 + 5b^3)\lambda^2) \sinh(\lambda a - \lambda r_0) \} \quad (A76)$$

$$B_{13} = \frac{1}{5a^3b^3\lambda^4} \{ 6r_0(-30a + (-14a^3 + 12ab^2 + 5b^3)\lambda^2) \cosh(\lambda a) - 2(-90ar_0 + 3(10ab^3$$



$$\begin{aligned}
 &+(a^3 - 6ab^2 + 5b^3)r_0 - 10ar_0^3)\lambda^2 + (a^3 - 6ab^2 + 5b^3)(2a^3 + r_0^3)\lambda^4) \cosh(\lambda r_0) + 6r_0\lambda(a(30a \\
 &+(4a^3 - 12ab^2 + 5b^3)\lambda^2) \sinh(\lambda a) + r_0(-30a + (a^3 - 6ab^2 + 5b^3)\lambda^2) \sinh(\lambda r_0))\} \quad (A77)
 \end{aligned}$$

$$\begin{aligned}
 B_{14} = &\frac{-1}{5a^3b^3\lambda^4} \{6 r_0(a\lambda(30a + (4a^3 - 12ab^2 + 5b^3)\lambda^2) \cosh(\lambda a) + r_0\lambda(-30a + (a^3 \\
 &-6ab^2 + 5b^3)\lambda^2) \cosh(\lambda r_0) + (-30a + (-14a^3 + 12ab^2 + 5b^3)\lambda^2) \sinh(\lambda a)) - 2(-90ar_0 + 3(a^3r_0 \\
 &+ 5b^3r_0 + 2a(5b^3 - 3b^2r_0 - 5r_0^3))\lambda^2 + (a^3 - 6ab^2 + 5b^3)(2a^3 + r_0^3)\lambda^4) \sinh(\lambda r_0)\} \quad (A78)
 \end{aligned}$$

$$\begin{aligned}
 B_{15} = &\frac{1}{75b^3} \{-30 (a^3 + 2b^3)r_0\lambda + \lambda(60a^4 + 6ab^2(5b - 9r_0) + 15a^3r_0 - 45a^2r_0^2 + 6b^2r_0(5b + 9r_0) \\
 &+(5a^3 - 18ab^2 + 10b^3)(2a^3 + r_0^3)\lambda^2) \cosh(\lambda a - \lambda r_0) - 3(20a^3 + 10b^3 + 15a^2r_0 - 18b^2r_0 \\
 &+(2a^3(5a^2 - 6b^2) + (-5a^3 + 18ab^2 - 10b^3)r_0^2 + (5a^2 - 6b^2)r_0^3)\lambda^2) \sinh(\lambda a - \lambda r_0)\} \quad (A79)
 \end{aligned}$$

$$\begin{aligned}
 B_{16} = &\frac{a^5}{25b^6} \{\lambda(3(a - r_0)r_0 + a(2a^3 + r_0^3)\lambda^2) \cosh(\lambda a - \lambda r_0) - (3r_0 + (2a^3 - 3ar_0^2 \\
 &+ r_0^3)\lambda^2) \sinh(\lambda a - \lambda r_0)\} \quad (A80)
 \end{aligned}$$

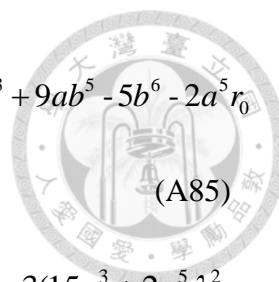
$$\begin{aligned}
 B_{17} = &\frac{2r_0}{5b^6\lambda^2} \{2a^3(a^3 - b^3)\lambda^3 + (2a^3 + b^3)(-\lambda(-3r_0 + a(3 + r_0^2\lambda^2))) \cosh(\lambda a - \lambda r_0) \\
 &+(3 + r_0(-3a + r_0)\lambda^2) \sinh(\lambda a - \lambda r_0)\} \quad (A81)
 \end{aligned}$$

$$\begin{aligned}
 B_{18} = &\frac{2a^3}{5b^6} \{(a^3 - b^3)r_0\lambda + (2a^3 + b^3)(a\lambda \cosh(\lambda a - \lambda r_0) - \sinh(\lambda a - \lambda r_0))\} \quad (A82)
 \end{aligned}$$

$$\begin{aligned}
 B_{19} = &\frac{-2}{5b^6\lambda^2} \{(a^3 - b^3)(3r_0 + (2a^3 + r_0^3)\lambda^2) \cosh(\lambda r_0) - 3(2a^3 + b^3)r_0(-\cosh(\lambda a) \\
 &+ a\lambda \sinh(\lambda a)) + 3(-a^3 + b^3)r_0^2\lambda \sinh(\lambda r_0)\} \quad (A83)
 \end{aligned}$$

$$\begin{aligned}
 B_{20} = &\frac{1}{5b^6\lambda^2} \{-6 a(2a^3 + b^3)r_0\lambda \cosh(\lambda a) + 6(2a^3 + b^3)r_0 \sinh(\lambda a) + 2(a^3 \\
 &-b^3)(-3 r_0^2\lambda \cosh(r_0\lambda) + (3r_0 + (2a^3 + r_0^3)\lambda^2) \sinh(\lambda r_0))\} \quad (A84)
 \end{aligned}$$

$$\begin{aligned}
 B_{21} = &\frac{4r_0}{15a^2b^6\lambda^4} \{15 (-2a^6 + a^3b^3 + b^6)\lambda^3 + \lambda(135a^3(a - r_0) + 3(a^6 - 5a^3b^3 + 9ab^5 \\
 &-6a^5r_0 + 15a^2b^3r_0 + 15a^4r_0^2 - b^5(5b + 9r_0))\lambda^2 + (a^6 - 5a^3b^3 + 9ab^5 - 5b^6)r_0^2\lambda^4) \cosh(\lambda a - \lambda r_0)
 \end{aligned}$$



$$\begin{aligned}
 &+3(-45a^3 - 3(2a^5 - 5a^2b^3 + 3b^5 - 15a^4r_0 + 5a^3r_0^2)\lambda^2 + r_0(a^6 - 5a^3b^3 + 9ab^5 - 5b^6 - 2a^5r_0 \\
 &+ 5a^2b^3r_0 - 3b^5r_0)\lambda^4) \sinh(\lambda a - \lambda r_0) \} \tag{A85}
 \end{aligned}$$

$$\begin{aligned}
 B_{22} = &\frac{-4a}{15b^6\lambda^2} \{ \lambda(45a^4 + (a^6 - 5a^3b^3 + 9ab^5 - 5b^6)\lambda^2) \cosh(\lambda a - \lambda r_0) - 3(15a^3 + 2a^5\lambda^2 \\
 &- 5a^2b^3\lambda^2 + 3b^5\lambda^2) \sinh(\lambda a - \lambda r_0) \} \tag{A86}
 \end{aligned}$$

$$\begin{aligned}
 B_{23} = &\frac{-4}{5a^2b^6\lambda^4} \{ -3r_0(15a^3 + 2a^5\lambda^2 - 5a^2b^3\lambda^2 + 3b^5\lambda^2) \cosh(\lambda a) + \lambda(5(-2a^6 + a^3b^3 \\
 &+ b^6)\lambda \cosh(\lambda r_0) + r_0(45a^4 + (a^6 - 5a^3b^3 + 9ab^5 - 5b^6)\lambda^2) \sinh(\lambda a)) \} \tag{A87}
 \end{aligned}$$

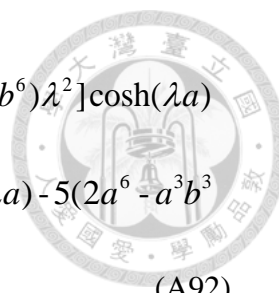
$$\begin{aligned}
 B_{24} = &\frac{4}{5a^2b^6\lambda^4} \{ r_0\lambda(45a^4 + (a^6 - 5a^3b^3 + 9ab^5 - 5b^6)\lambda^2) \cosh(\lambda a) - 3r_0(15a^3 + 2a^5\lambda^2 \\
 &- 5a^2b^3\lambda^2 + 3b^5\lambda^2) \sinh(\lambda a) + 5(-2a^6 + a^3b^3 + b^6)\lambda^2 \sinh(\lambda r_0) \} \tag{A88}
 \end{aligned}$$

$$\begin{aligned}
 B_{25} = &\frac{4r_0}{15a^5b^6\lambda^4} \{ \lambda(45(2a^6 - 4a^3b^3 - b^6)(a - r_0) + 3a(2a^8 - 10a^5b^3 - 12a^7r_0 + 30a^4b^3r_0 \\
 &+ 10a^6r_0^2 - 5b^6r_0^2 - 2a^2b^5(5b + 9r_0) + 2a^3(9b^5 - 10b^3r_0^2))\lambda^2 + 2a^3(a^6 - 5a^3b^3 + 9ab^5 \\
 &- 5b^6)r_0^2\lambda^4) \cosh(\lambda a - \lambda r_0) + 3(15(-2a^6 + 4a^3b^3 + b^6) + (-12a^8 + 30a^5b^3 + 30a^7r_0 - 60a^4b^3r_0 \\
 &- 15ab^6r_0 - 10a^6r_0^2 + 5b^6r_0^2 + a^3(-18b^5 + 20b^3r_0^2))\lambda^2 + 2a^3r_0(a^6 - 5a^3b^3 + 9ab^5 - 2a^5r_0 + 5a^2b^3r_0 \\
 &- b^5(5b + 3r_0))\lambda^4) \sinh(\lambda a - \lambda r_0) \} \tag{A89}
 \end{aligned}$$

$$\begin{aligned}
 B_{26} = &\frac{-1}{15a^2b^6\lambda^2} \{ 60(-2a^6 + a^3b^3 + b^6)r_0\lambda + 4a\lambda(15(2a^6 - 4a^3b^3 - b^6) + 2a^2(a^6 \\
 &- 5a^3b^3 + 9ab^5 - 5b^6)\lambda^2) \cosh(\lambda a - \lambda r_0) - 12(10a^6 - 5b^6 + 4a^8\lambda^2 - 10a^5b^3\lambda^2 + a^3(-20b^3 \\
 &+ 6b^5\lambda^2)) \sinh(\lambda a - \lambda r_0) \} \tag{A90}
 \end{aligned}$$

$$\begin{aligned}
 B_{27} = &\frac{4r_0}{5a^5b^6\lambda^4} \{ 3[10a^6 - 5b^6 + 4a^8\lambda^2 - 10a^5b^3\lambda^2 + a^3(-20b^3 + 6b^5\lambda^2)] \cosh(\lambda a) \\
 &+ a\lambda(15(-2a^6 + 4a^3b^3 + b^6) - 2a^2(a^6 - 5a^3b^3 + 9ab^5 - 5b^6)\lambda^2) \sinh(\lambda a) \\
 &- 5(2a^6 - a^3b^3 - b^6)[(3 + r_0^2\lambda^2) \cosh(\lambda r_0) - 3r_0\lambda \sinh(\lambda r_0)] \} \tag{A91}
 \end{aligned}$$





$$B_{28} = \frac{-4r_0}{5a^5b^6\lambda^4} \{ a\lambda[15(-2a^6 + 4a^3b^3 + b^6) - 2a^2(a^6 - 5a^3b^3 + 9ab^5 - 5b^6)\lambda^2] \cosh(\lambda a) + 3[10a^6 - 5b^6 + 4a^8\lambda^2 - 10a^5b^3\lambda^2 + a^3(-20b^3 + 6b^5\lambda^2)] \sinh(\lambda a) - 5(2a^6 - a^3b^3 - b^6)[-3r_0\lambda \cosh(\lambda r_0) + (3 + r_0^2\lambda^2) \sinh(\lambda r_0)] \} \quad (A92)$$

$$B_{29} = \frac{1}{5b^6\lambda^2} \{ 2(a^3 - b^3)[3r_0 + (2a^3 + r_0^3)\lambda^2] \cosh(\lambda r_0) - 6(2a^3 + b^3)r_0[-\cosh(\lambda a) + a\lambda \sinh(\lambda a)] + 6(-a^3 + b^3)r_0^2\lambda \sinh(\lambda r_0) \} \quad (A93)$$

$$B_{30} = \frac{4r_0}{5a^5b^6\lambda^4} \{ 3[10a^6 - 5b^6 + 4a^8\lambda^2 - 10a^5b^3\lambda^2 + a^3(-20b^3 + 6b^5\lambda^2)] \cosh(\lambda a) + a\lambda(15(-2a^6 + 4a^3b^3 + b^6) - 2a^2(a^6 - 5a^3b^3 + 9ab^5 - 5b^6)\lambda^2) \sinh(\lambda a) - 5(2a^6 - a^3b^3 - b^6)[(3 + r_0^2\lambda^2) \cosh(\lambda r_0) - 3r_0\lambda \sinh(\lambda r_0)] \} \quad (A94)$$

$$B_{31} = \frac{-4}{5a^2b^6\lambda^4} \{ -3r_0(15a^3 + 2a^5\lambda^2 - 5a^2b^3\lambda^2 + 3b^5\lambda^2) \cosh(\lambda a) + \lambda[5(-2a^6 + a^3b^3 + b^6)\lambda \cosh(\lambda r_0) + r_0(45a^4 + (a^6 - 5a^3b^3 + 9ab^5 - 5b^6)\lambda^2) \sinh(\lambda a)] \} \quad (A95)$$

$$B_{32} = \frac{-4}{5a^5b^6\lambda^7} \{ \cosh(\lambda r_0)(3(45a^3r_0 + (10a^6 + 6a^5r_0 - 15a^2b^3r_0 + b^5(-5b + 9r_0)) + 5a^3(-4b^3 + 3r_0^3))\lambda^2 + (a - b)^2(2a^3 + 4a^2b + 6ab^2 + 3b^3)(2a^3 + r_0^3)\lambda^4) \cosh(\lambda a) - \lambda(135a^4r_0 + 3(10a^7 + a^6r_0 - 5a^3b^3r_0 - 5b^6r_0 + ab^5(-5b + 9r_0) + 5a^4(-4b^3 + 3r_0^3))\lambda^2 + (a - b)^3(a^3 + 3a^2b + 6ab^2 + 5b^3)(2a^3 + r_0^3)\lambda^4) \sinh(\lambda a) + 3r_0^2\lambda(-3(15a^3 + 2a^5\lambda^2 - 5a^2b^3\lambda^2 + 3b^5\lambda^2) \cosh(\lambda a) + \lambda(45a^4 + (a^6 - 5a^3b^3 + 9ab^5 - 5b^6)\lambda^2) \sinh(\lambda a)) \sinh(\lambda r_0) \} \quad (A96)$$

$$B_{33} = \frac{-4}{5a^5b^6\lambda^7} \{ 15(2a^6 - a^3b^3 - b^6)r_0\lambda^3 + 3r_0^2\lambda \cosh(\lambda r_0)(3(15a^3 + 2a^5\lambda^2 - 5a^2b^3\lambda^2 + 3b^5\lambda^2) \cosh(\lambda a) - \lambda(45a^4 + (a^6 - 5a^3b^3 + 9ab^5 - 5b^6)\lambda^2) \sinh(\lambda a)) + (-3(45a^3r_0 + (10a^6 + 6a^5r_0 - 15a^2b^3r_0 + b^5(-5b + 9r_0)) + 5a^3(-4b^3 + 3r_0^3))\lambda^2 + (a - b)^2(2a^3 + 4a^2b + 6ab^2 + 3b^3)(2a^3 + r_0^3)\lambda^4) \cosh(\lambda a) + \lambda(135a^4r_0 + 3(10a^7 + a^6r_0 - 5a^3b^3r_0 - 5b^6r_0 + ab^5(-5b + 9r_0)) \sinh(\lambda a) \} \quad (A97)$$



$$+5a^4(-4b^3+3r_0^3))\lambda^2+(a-b)^3(a^3+3a^2b+6ab^2+5b^3)(2a^3+r_0^3)\lambda^4)\sinh(\lambda a))\sinh(\lambda r_0)\} \quad (\text{A97})$$

$$B_{34} = \frac{-2}{5b^6\lambda^2}\{-3a(2a^3+b^3)r_0\lambda\cosh(\lambda a)+3(2a^3+b^3)r_0\sinh(\lambda a) \\ +(a^3-b^3)(-3r_0^2\lambda\cosh(\lambda r_0)+(3r_0+(2a^3+r_0^3)\lambda^2)\sinh(\lambda r_0))\} \quad (\text{A98})$$

$$B_{35} = \frac{-4r_0}{5a^5b^6\lambda^4}\{a\lambda(15(-2a^6+4a^3b^3+b^6)-2a^2(a^6-5a^3b^3+9ab^5-5b^6)\lambda^2)\cosh(\lambda a) \\ +3(10a^6-5b^6+4a^8\lambda^2-10a^5b^3\lambda^2+a^3(-20b^3+6b^5\lambda^2))\sinh(\lambda a)\} \quad (\text{A99})$$

$$B_{36} = \frac{4}{5a^2b^6\lambda^4}\{r_0\lambda(45a^4+(a^6-5a^3b^3+9ab^5-5b^6)\lambda^2)\cosh(\lambda a)-3r_0(15a^3+2a^5\lambda^2 \\ -5a^2b^3\lambda^2+3b^5\lambda^2)\sinh(\lambda a)+5(-2a^6+a^3b^3+b^6)\lambda^2\sinh(\lambda r_0)\} \quad (\text{A100})$$

$$B_{37} = \frac{-1}{5a^5b^6\lambda^7}\{60(-2a^6+a^3b^3+b^6)r_0\lambda^3+4\cosh(\lambda r_0)(\lambda(135a^4r_0+3(10a^7+a^6r_0 \\ -5a^3b^3r_0-5b^6r_0+ab^5(-5b+9r_0))+5a^4(-4b^3+3r_0^3))\lambda^2+(a-b)^3(a^3+3a^2b+6ab^2+5b^3)(2a^3 \\ +r_0^3)\lambda^4)\cosh(\lambda a)-3(45a^3r_0+(10a^6+6a^5r_0-15a^2b^3r_0+b^5(-5b+9r_0))+5a^3(-4b^3 \\ +3r_0^3))\lambda^2+(a-b)^2(2a^3+4a^2b+6ab^2+3b^3)(2a^3+r_0^3)\lambda^4)\sinh(\lambda a)) \\ +12r_0^2\lambda(-\lambda(45a^4+(a^6-5a^3b^3+9ab^5-5b^6)\lambda^2)\cosh(\lambda a)+3(15a^3+2a^5\lambda^2 \\ -5a^2b^3\lambda^2+3b^5\lambda^2)\sinh(\lambda a))\sinh(\lambda r_0)\} \quad (\text{A101})$$

$$B_{38} = \frac{-4}{5a^5b^6\lambda^7}\{3r_0^2\lambda\cosh(\lambda r_0)(\lambda(45a^4+(a^6-5a^3b^3+9ab^5-5b^6)\lambda^2)\cosh(\lambda a) \\ -3(15a^3+2a^5\lambda^2-5a^2b^3\lambda^2+3b^5\lambda^2)\sinh(\lambda a))+(-\lambda(135a^4r_0+3(10a^7+a^6r_0-5a^3b^3r_0 \\ -5b^6r_0+ab^5(-5b+9r_0))+5a^4(-4b^3+3r_0^3))\lambda^2+(a-b)^3(a^3+3a^2b+6ab^2 \\ +5b^3)(2a^3+r_0^3)\lambda^4)\cosh(\lambda a)+3(45a^3r_0+(10a^6+6a^5r_0-15a^2b^3r_0+b^5(-5b+9r_0))+5a^3(-4b^3 \\ +3r_0^3))\lambda^2+(a-b)^2(2a^3+4a^2b+6ab^2+3b^3)(2a^3+r_0^3)\lambda^4)\sinh(\lambda a))\sinh(\lambda r_0)\} \quad (\text{A102})$$

for the Kuwabara model.

## Biographical Sketch



Hsuan-Chiao Liu was born in Nantou on October 11, 1990. He graduated from Rangitoto College in New Zealand in the summer of 2009, and then entered the Department of Chemical and Material Engineering of Chang Gung University in the next year. After earning his Bachelor's Degree in 2014, he continued his advanced study in the graduate school at the Department of Chemical Engineering of National Taiwan University for a Master Degree up to the present.